27 Chade AR, Lerman A, Lerman LO. Kidney in early atherosclerosis. *Hypertension* 2005; **45**: 1042–1049.
28 Rothermund L, Lorenz M, Schnieber A, Eberson J, Bauhaus I, Bernhard Haug M, Schulz A, Keller F, Vetter R, Kreutz R. Impact of nephron number dosing on cardiorenal damage and effects of ACE inhibition. *Am J Hypertens* 2010; **24**: 474–481.
29 Singh RR, Denton KM, Bertram JF, Jefferies AJ, Head GA, Lombardo P, Schneider-Kolsky M, Moritz KM. Development of cardiovascular disease due to renal insufficiency in male sheep following fetal unilateral nephrectomy. *J Hypertens* 2009; **27**: 386–396.
30 Hollenberg NK, Adams DF, Solomon HS, Rashid A, Abrams HL, Merrill JP. Senescence and the renal vasculature in normal man. *Circ Res* 1974; **34**: 309–316.
31 Watanabe S, Okura T, Liu J, Miyoshi K, Fukuoka T, Hiwada K, Higaki J. Serum cystatin C level is a marker of end-organ damage in patients with essential hypertension. *Hypertens Res* 2003; **26**: 895–899.
32 Perticone F, Maio R, Ruberto C, Cassano S, Tripepi G, Perticone M, Sesti G, Zoccali C. Kidney function and risk factors for left ventricular hypertrophy in untreated uncomplicated essential hypertension. *Am J Kidney Dis* 2008; **52**: 74–84.
33 Ito S. Cardiorenal connection in chronic kidney disease. *Clin Exp Nephrol* 2012; **16**: 8–16.
34 Kasiske BL. Relationship between vascular disease and age-associated changes in the human kidney. *Kidney Int* 1987; **31**: 1153–1159.

Supplementary Information accompanies the paper on Hypertension Research website (http://www.nature.com/hr)

Am J Physiol Renal Physiol 306: F1418–F1428, 2014.
First published May 7, 2014; doi:10.1152/ajprenal.00633.2013.

Phosphate overload directly induces systemic inflammation and malnutrition as well as vascular calcification in uremia

Shunsuke Yamada,[1,3] Masanori Tokumoto,[3] Narihito Tatsumoto,[1] Masatomo Taniguchi,[1] Hideko Noguchi,[1] Toshiaki Nakano,[1] Kosuke Masutani,[1] Hiroaki Ooboshi,[3] Kazuhiko Tsuruya,[1,2] and Takanari Kitazono[1]

[1]*Department of Medicine and Clinical Science, Graduate School of Medical Sciences, Kyushu University, Fukuoka, Japan;* [2]*Department of Integrated Therapy for Chronic Kidney Disease, Graduate School of Medical Sciences, Kyushu University, Fukuoka, Japan; and* [3]*Department of Internal Medicine, Fukuoka Dental College Medical and Dental Hospital, Fukuoka, Japan*

Submitted 27 November 2013; accepted in final form 2 May 2014

Yamada S, Tokumoto M, Tatsumoto N, Taniguchi M, Noguchi H, Nakano T, Masutani K, Ooboshi H, Tsuruya K, Kitazono T. Phosphate overload directly induces systemic inflammation and malnutrition as well as vascular calcification in uremia. *Am J Physiol Renal Physiol* 306: F1418–F1428, 2014. First published May 7, 2014; doi:10.1152/ajprenal.00633.2013.—Hyperphosphatemia contributes to increased cardiovascular mortality through vascular calcification (VC) in patients with chronic kidney disease (CKD). Malnutrition and inflammation are also closely linked to an increased risk of cardiovascular death in CKD. However, the effects of P_i overload on inflammation and malnutrition remain to be elucidated. The aim of the present study was to investigate the effects of dietary P_i loading on the interactions among inflammation, malnutrition, and VC in CKD. We used control rats fed normal diets and adenine-induced CKD rats fed diets with different P_i concentrations ranging from 0.3% to 1.2% for 8 wk. CKD rats showed dietary P_i concentration-dependent increases in serum and tissue levels of TNF-α and urinary and tissue levels of oxidative stress markers and developed malnutrition (decrease in body weight, serum albumin, and urinary creatinine excretion), VC, and premature death without affecting kidney function. Treatment with 6% lanthanum carbonate blunted almost all changes induced by P_i overload. Regression analysis showed that serum P_i levels closely correlated with the extent of inflammation, malnutrition, and VC. Also, in cultured human vascular smooth muscle cells, high-P_i medium directly increased the expression of TNF-α in advance of the increase in osteochondrogenic markers. Our data suggest that dietary P_i overload induces systemic inflammation and malnutrition, accompanied by VC and premature death in CKD, and that inhibition of P_i loading through dietary or pharmacological interventions or anti-inflammatory therapy may be a promising treatment for the prevention of malnutrition-inflammation-atherosclerosis syndrome.

chronic kidney disease; inflammation; malnutrition; phosphate; vascular calcification; malnutrition-inflammation-atherosclerosis syndrome

HYPERPHOSPHATEMIA, which is highly prevalent in patients with chronic kidney disease (CKD), is the manifestation of the relative P_i overload due to decreased P_i clearance in CKD (12). Mounting evidence has revealed that hyperphosphatemia contributes to increased cardiovascular and all-cause mortality in CKD patients, which is considered to be mediated by vascular calcification (VC) (4, 23). Both clinical and preclinical studies have shown that dietary P_i restriction and P_i binder use can prevent hyperphosphatemia and retard the progression of VC, thereby lowering the mortality rate in CKD (13, 16, 31), suggesting the importance of maintaining an appropriate P_i balance in the management of CKD patients.

Another important disorder of CKD is malnutrition-inflammation-atherosclerosis (MIA) syndrome, a recently identified missing piece that partly explains the high cardiovascular mortality rate in CKD patients (25, 41, 42, 48). Clinical studies have reported that CKD is associated with elevated levels of inflammatory markers (3, 37) and that chronic inflammation in CKD promotes malnutrition and atherosclerosis (42). Furthermore, malnutrition has been reported to induce chronic inflammation (17). Accordingly, malnutrition and inflammation form a vicious cycle in CKD, leading to the development of cardiovascular disorders, VC, and subsequently increased mortality.

Recent experimental studies have revealed the underlying mechanisms by which P_i directly impairs the cardiovascular system (15, 39, 43). Hyperphosphatemia induces VC via transdifferentiation of vascular smooth muscle cells (VSMCs) into osteoblast-like cells and via apoptosis of VSMCs, which is triggered by P_i entry into cells through P_i transporter (Pit)-1 (15, 35, 43). Hyperphosphatemia also promotes endothelial dysfunction via impairment of nitric oxidase synthesis (39). Given that Pit-1 is expressed ubiquitously (44), it is plausible to speculate that excessive P_i loading has harmful effects not only on the cardiovascular system but also on other tissues, probably via inflammation and malnutrition, that may account for the development of several CKD-related disorders. However, studies focused on the potential influence of P_i overload on the interactions among inflammation, malnutrition, and VC are lacking.

Based on the above background, it was hypothesized that P_i overload is located on the upstream of MIA syndrome and triggers multistep inflammation, oxidative stress, malnutrition, and atherosclerosis (arterial medial calcification) cascades, leading to premature death in uremic milieu. To investigate this hypothesis, the effects of P_i overload on inflammation and malnutrition as well as VC in adenine-fed uremic rats and on cultured human VSMCs and HepG2 cells were examined. Our main objective was to clarify whether P_i loading is directly involved in the development of chronic inflammation and malnutrition in uremia.

METHODS

Cell cultures. Human umbilical arterial smooth muscle cells (HUASMCs) and HepG2 cells (a frequently used human liver hepatocytoma cell line for examining hepatocyte biology) were grown in a humidified 5% CO_2 incubator at 37°C in DMEM containing 4.5 g/l

Address for reprint requests and other correspondence: K. Tsuruya, Dept. of Integrated Therapy for Chronic Kidney Disease, Graduate School of Medical Sciences, Kyushu Univ., 3-1-1 Maidashi, Higashi-ku, Fukuoka 812-8582, Japan (e-mail: tsuruya@intmed2.med.kyushu-u.ac.jp).

glucose supplemented with 10% FBS, 10 mM sodium pyruvate, and 1% penicillin-streptomycin. Media were changed every 2 days. Cells were cultured on 12-well plates and grown until confluency. After reaching confluency, HUASMCs and HepG2 cells were cultured in DMEM with either of the following P_i concentrations: 0.9 mM (normal P_i concentration) or 2.9 mM (high P_i concentration). The P_i concentration was adjusted by the mixture of Na_2HPO_4 and NaH_2PO_4. On *day 1* after exposure to each medium, total RNA was extracted and used for real-time PCR for the determination of relative mRNA expression.

Animals and materials. All protocols were reviewed and approved by the Committee on Ethics of Animal Experiments of Kyushu University Faculty of Medicine (A23-198-0). Male Sprague-Dawley rats (10 wk old) were purchased from Kyudo (Saga, Japan). Animals were housed in a climate-controlled space with a 12:12-h day-night cycle and allowed free access to food and water. Standard diet (1.0% Ca^{2+} and 1.2% P_i, Oriental Yeast, Tokyo, Japan) was used as the diet for control rats and for all rats during the acclimatization period.

It has been a challenge to create a uremic animal model that consistently develops extensive arterial medial calcification without genetic manipulation (2, 38). To create such a rat model, a new rodent diet was used that modified the conventional adenine-based diet in the following three ways. First, a 0.3% adenine diet was used to slow the progression of CKD; a 0.75% adenine diet induces severe and rapid renal failure, leading to high mortality in 4–6 wk (51). Second, a casein-based diet was selected for the protein source because it can promote Ca^{2+} and P_i absorption from the gastrointestinal tract (26). Finally, 20% lactose was added to the diet to further enhance Ca^{2+} and P_i absorption from the gastrointestinal tract (19). This synthetic rodent diet provided a rat model exhibiting extensive and robust arterial medial calcification with a relatively longer lifespan, enabling researchers to investigate the complex mechanisms of arterial medial calcification in uremia. All synthetic rodent diets were purchased from Oriental Yeast.

Experimental protocols. Male Sprague-Dawley rats (n = 66) were fed the standard diet for 7 days to acclimatize. On *day 1*, rats were randomly subdivided into the following six groups, and each group was fed one of the specific diets for 8 wk (until *day 56*): control rats (CNT group; 1.2% P_i, n = 10), CKD rats fed a low-P_i diet (CKD-LP group; 0.3% P_i, n = 10), CKD rats fed a moderate-P_i diet (CKD-MP group; 0.6% P_i, n = 10), CKD rats fed a high-P_i diet (CKD-HP group; 0.9% P_i, n = 12), CKD rats fed an extremely high-P_i diet (CKD-EP group; 1.2% P_i, n = 14), and CKD rats fed an extremely high-P_i diet and 6% lanthanum carbonate (CKD-LaC group; 1.2% P_i, n = 10). Diets in the CKD groups contained 0.3% adenine to induce renal failure and 1.0% Ca^{2+}, 20% lactose, and 19% casein-based protein to accelerate intestinal Ca^{2+} and P_i absorption. The diet in the CNT group contained 1.0% Ca^{2+}, 1.2% P_i, and 19% grain-based protein but did not contain lactose. The content of each diet is shown in Table 1.

Every 2 wk, rats were housed in metabolic cages for 24 h, and food intake and urine volume were recorded. The systolic blood pressure level was monitored in the conscious state using the tail-cuff method (BP monitor MK-2000, Muromachi Kikai, Tokyo, Japan) at *weeks 2*, *4*, and *6* in each group. Collected urine was centrifuged at 3,000 *g* for 15 min, and the supernatant was stored at −30°C until analysis. At euthanization (after 8 wk), the blood, aorta, kidney, heart, and liver were collected. Serum was separated by centrifugation at 5,000 *g* and stored at −80°C until analysis. The aorta was weighed using a microbalance. The aorta, heart, kidney, and liver were dissected into several samples. One sample was immersed in formalin for histological analysis; the others were stored at −80°C until later analyses.

Biochemical parameters. Serum and urinary levels of Ca^{2+}, P_i, albumin, and creatinine (Cr) were measured with an automated analyzer (Hitachi, Tokyo, Japan). Cr clearance was determined using the standard method: urinary Cr concentration × urine volume/serum Cr concentration/1,440 (ml/min). The following biochemical parameters were determined by commercially available rat ELISA kits: intact parathyroid hormone (Immutopics, San Clemente, CA), serum calcitriol (Wuhan EIAab Science, Wuhan, China), serum intact FGF_{23} (Kainos Laboratories, Tokyo, Japan), serum fetuin-A (Wuhan EIAab Science), urinary 8-hydroxy-2′-deoxyguanosine (8-OHdG; JaICA, Shizuoka, Japan), and serum TNF-α (R&D Systems). All kits were used according to the manufacturers' instructions, and their qualities were within analytic levels.

Examination of arterial medial calcification and kidneys. Four-micrometer sections from the paraffin-embedded aorta were deparaffinized and processed for von Kossa staining using the standard method. To evaluate the degree of aortic medial calcification quantitatively, frozen aortic tissue was weighed and then hydrolyzed in 1 ml hydrochloride (6 mol/l) for 24 h. The Ca^{2+} content of the supernatant was determined by the *o*-cresolphthalein complexone method using a commercially available kit (Calcium E-test, Wako, Osaka, Japan) and normalized to wet tissue weight (in μg/mg wet wt). Digital micrographs of the stained aorta were captured on an Eclipse E800 microscope (Nikon, Tokyo, Japan). For kidneys, 4-μm sections from paraffin-embedded kidneys were deparaffinized and processed using Masson trichrome staining using the standard method.

Immunohistochemistry. Four-micrometer sections from the paraffin-embedded aorta were deparaffinized, rehydrated, and prepared for antigen retrieval. Antigen retrieval was performed using a microwave for 15 min in citrate buffer (pH 6) or with 0.1% proteinase K solution for 20 min. Inactivation of intrinsic peroxidase was then performed by incubation in 0.3% H_2O_2. To reduce nonspecific background staining, sections were treated with 5% skim milk for 30 min at room temperature and then incubated in a humidified chamber for 1 h at 37°C with the following primary antibodies: rabbit polyclonal anti-phosphorylated-NF-κB p65 (Ser^{276}, diluted 1:50, Santa Cruz Biotechnology, Santa Cruz, CA) and mouse monoclonal anti-8-OHdG (diluted 1:200, JaICA). After being washing with PBS and Tween 20 [0.2% (vol/vol)] for 5 min three times, sections were incubated with secondary antibody with peroxidase (4 μg/ml, Nichirei, Tokyo, Japan) for 30 min at room temperature. Horseradish peroxidase was visualized by a reaction with 3,3′-diaminobenzidine tetrahydrochloride and H_2O_2. Digital micrographs of the immunohistochemistry were captured on an Eclipse E800 microscope (Nikon). Immunohistochemically stained

Table 1. *Content of the animal diets*

Group	Ca^{2+}, %	P_i, %	Protein	Lactose, %	Adenine, %	Lanthanum Carbonate, %
CNT	1.0	1.2	19% (grain based)	0	0	0
CKD-LP	1.0	0.3	19% (casein based)	20	0.3	0
CKD-MP	1.0	0.6	19% (casein based)	20	0.3	0
CKD-HP	1.0	0.9	19% (casein based)	20	0.3	0
CKD-EP	1.0	1.2	19% (casein based)	20	0.3	0
CKD-LaC	1.0	1.2	19% (casein based)	20	0.3	6

On *day 1*, rats were randomly subdivided into the following six groups, and each group was fed one of the specific diets for 8 wk (until *day 56*): control rats (CNT group; 1.2% P_i, n = 10), CKD rats fed a low-P_i diet (CKD-LP group; 0.3% P_i, n = 10), CKD rats fed a moderate-P_i diet (CKD-MP group; 0.6% P_i, n = 10), CKD rats fed a high-P_i diet (CKD-HP group; 0.9% P_i, n = 12), CKD rats fed an extremely high-P_i diet (CKD-EP group; 1.2% P_i, n = 14), and CKD rats fed an extremely high-P_i diet and 6% lanthanum carbonate (CKD-LaC group; 1.2% P_i, n = 10). Diets in the CKD groups contained 0.3% adenine.

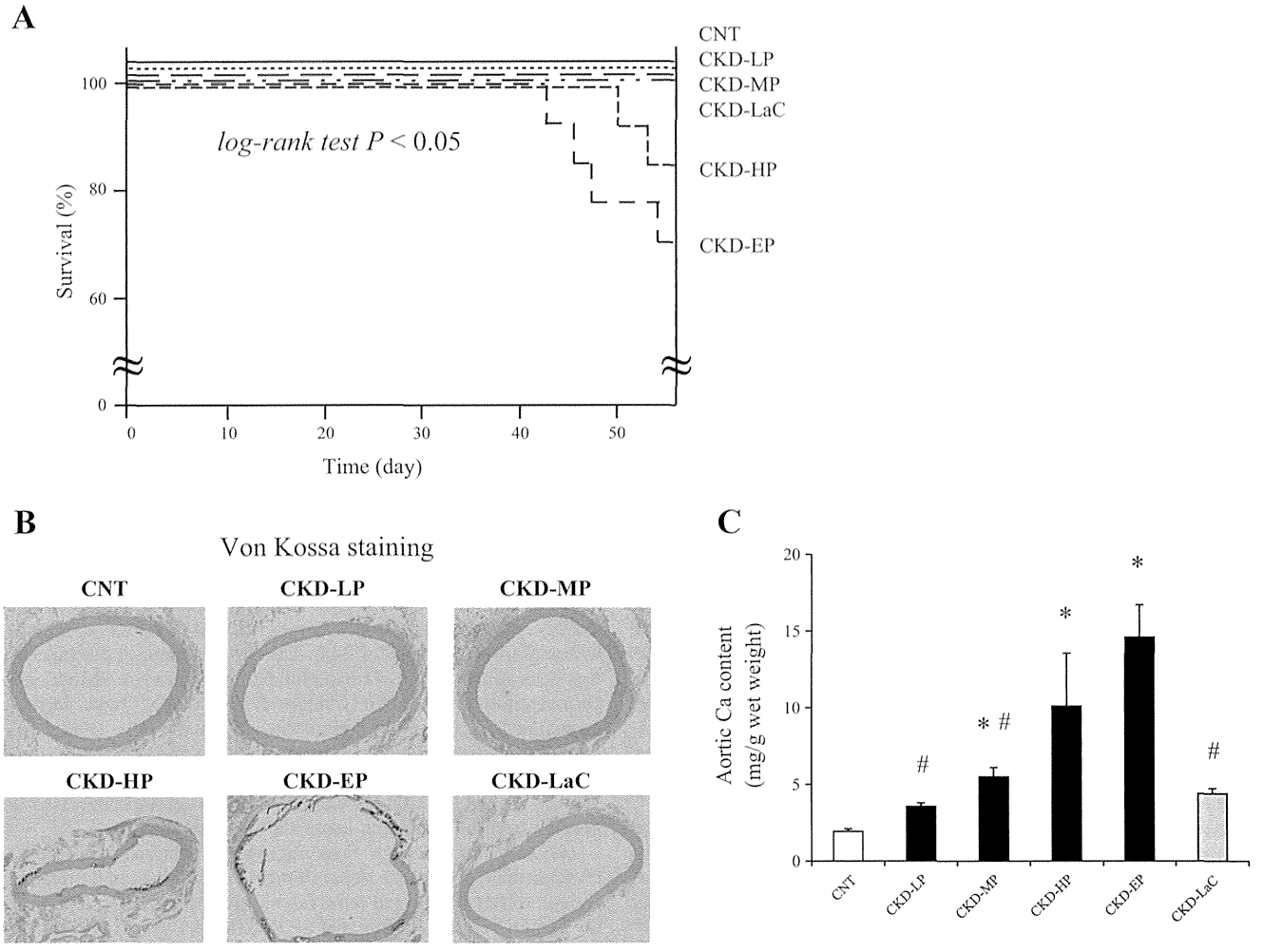

Fig. 1. Effects of dietary P_i loading on survival and vascular calcification. *A*: the Kaplan-Meier method and log-rank test were used to compare survival among groups. *B*: representative photomicrographs of the abdominal aorta stained with von Kossa. Original magnification: ×40. *C*: quantification of Ca^{2+} content in the abdominal aorta. On *day 1*, rats were randomly subdivided into the following six groups, and each group was fed one of the specific diets for 8 wk (until *day 56*): control rats (CNT group; 1.2% P_i, $n = 10$), rats with chronic kidney disease (CKD) fed a low-P_i diet (CKD-LP group; 0.3% P_i, $n = 10$), CKD rats fed a moderate-P_i diet (CKD-MP group; 0.6% P_i, $n = 10$), CKD rats fed a high-P_i diet (CKD-HP group; 0.9% P_i, $n = 12$), CKD rats fed an extremely high-P_i diet (CKD-EP group; 1.2% P_i, $n = 14$), and CKD rats fed an extremely high-P_i diet and 6% lanthanum carbonate (CKD-LaC group; 1.2% P_i, $n = 10$). Diets in the CKD groups contained 0.3% adenine. Data are expressed as means ± SE. One-way ANOVA followed by the Tukey-Kramer test was performed. Two-tailed P values of <0.05 were considered statistically significant. *$P < 0.05$ vs. the CNT group; #$P < 0.05$ vs. the CKD-EP group.

areas for 8-OHdG were quantitatively assessed and expressed as arbitrary units using National Institutes of Health ImageJ software (http://rsb.info.nih.gov/ij/).

Real-time PCR. Total RNA was extracted from HUASMCs and HepG2 cells and frozen rat tissue in liquid nitrogen using TRIzol reagent (Invitrogen Life Technologies, Carlsbad, CA) using the guanidinium thocyanate phenol-chloroform method according to the manufacturer's instructions and used to prepare cDNA by reverse transcription using a PrimeScript RT reagent kit (Perfect Real Time, Takara Bio, Otsu, Japan). Real-time quantitative PCR was performed using SYBR Premix Ex Taq (Takara Bio), Applied Biosystems 7500 real-time PCR systems (Applied Biosystems), and the following primers purchased from Takara Bio: rat GAPDH, RA015380; rat TNF-α, RA043092; rat albumin, RA065413; rat fetuin-A, RA065433;

Table 2. *Serum and urinary biochemical parameters at week 8*

Parameters	CNT Group	CKD-LP Group	CKD-MP Group	CKD-HP Group	CKD-EP Group	CKD-LaC Group
Serum Ca^{2+}, mmol/l	2.50 ± 0.10	3.37 ± 0.15*†	3.19 ± 0.08*†	2.77 ± 0.20†	1.80 ± 0.55*	3.19 ± 0.10*†
Serum P_i, mmol/l	2.64 ± 0.10	1.94 ± 0.13†	3.07 ± 0.13†	4.65 ± 0.39*†	9.11 ± 0.32*	2.62 ± 0.13†
Serum intact parathyroid hormone, pg/ml	41.6 ± 4.7	35.8 ± 4.5†	202.1 ± 58.4*†	463.1 ± 110.5*	778.5 ± 116.6*	82.2 ± 14.2*†
Serum FGF_{23}, pg/ml	438 ± 33	5,186 ± 799†	30,188 ± 4,360*†	87,462 ± 23,662*	132,754 ± 32,513*	21,485 ± 7,404†
Serum calcitriol, pg/ml	95.4 ± 25.2	5.2 ± 1.4*†	5.1 ± 0.8*†	18.2 ± 4.0*	18.5 ± 5.2*	6.0 ± 1.9*†
Urinary P_i excretion, mg/day	0.6 ± 0.1	1.0 ± 0.4†	15.3 ± 0.8*†	49.3 ± 3.2*†	101.8 ± 4.2*	6.6 ± 1.0†

Data are means ± SE. Diets in the CKD groups contained 0.3% adenine. One-way ANOVA followed by the Tukey-Kramer test was performed. P values of <0.05 were considered statistically significant. *$P < 0.05$ vs. the CNT group; #$P < 0.05$ vs. the CKD-EP group.

Table 3. *Blood pressure levels at each week*

Parameters	CNT Group	CKD-LP Group	CKD-MP Group	CKD-HP Group	CKD-EP Group	CKD-LaC Group
Systolic blood pressure, mmHg						
Week 2	105 ± 3	109 ± 7	102 ± 3	111 ± 5	103 ± 4	110 ± 4
Week 4	103 ± 3	118 ± 4	110 ± 4	115 ± 4	106 ± 2	106 ± 3
Week 6	102 ± 7	103 ± 5	112 ± 4	110 ± 5	110 ± 7	112 ± 4

Data are means ± SE. Diets in the CKD groups contained 0.3% adenine.

rat Slc20a1 (Pit-1), RA011281; human GAPDH, HA607812; human albumin, HA118070; human fetuin-A, HA149248; human TNF-α, HA198263; human Klotho, HA148243; human NADPH oxidase 4 (Nox4), HA184575; and human bone morphogenetic protein-2, HA193805. The cycling condition was 30 s at 95°C followed by 40 cycles of 5 s at 95°C for denaturation and 40 s of annealing at 60°C. The specificity of the PCR products was confirmed by analysis of the melting curves and additionally by agarose gel electrophoresis. All measurements were performed in duplicate, and mRNA fold changes were calculated using the $2^{-\Delta\Delta C_t}$ method (where C_t is threshold cycle) using GADPH as an internal reference.

Statistical analysis. Statistical analyses were performed using JMP (version 10.0, SAS institute, Tokyo, Japan). Data are presented as means ± SE. Differences among groups were analyzed by an unpaired *t*-test for two groups and one-way ANOVA followed by a Tukey-Kramer test for more than three groups. Univariable and multivariable linear regression analyses were performed to determine correlations among parameters. For regression analysis, data from CKD-LP, CKD-MP, CKD-HP, and CKD-EP rats were used ($n = 40$). Serum Cr was used as the covariate in multivariable analysis. For all tests, two-tailed P values of <0.05 were considered statistically significant.

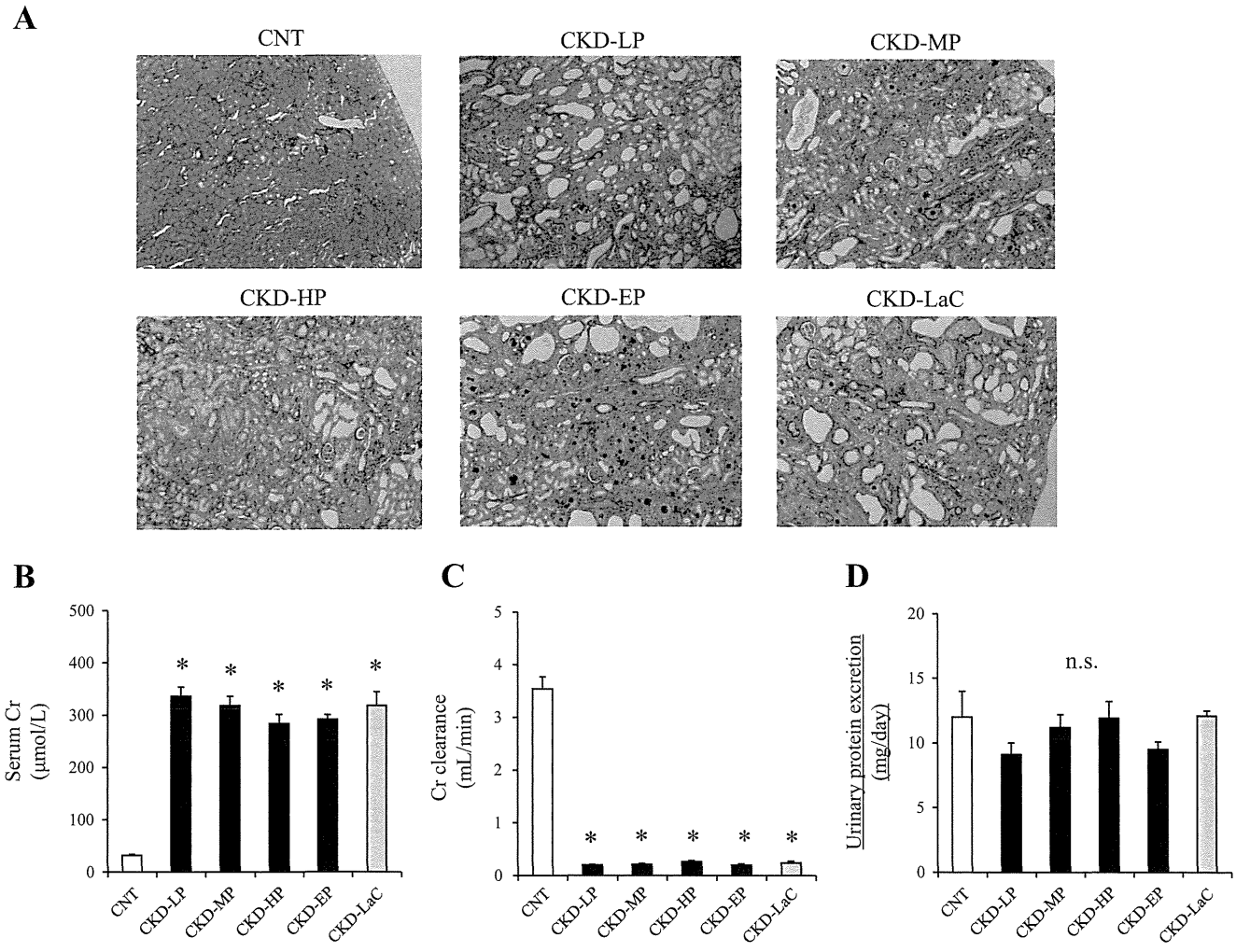

Fig. 2. Effects of dietary P_i loading on kidney histology, kidney function, and proteinuria. *A*: representative photomicrographs of the kidney stained by the Masson trichrome method in each group. Original magnification: ×100. *B*: serum creatinine (Cr). *C*: Cr clearance. *D*: urinary P_i excretion. n.s., not significant. CNT: P_i 1.2%; CKD-LP: P_i 0.3%; CKD-MP: P_i 0.6%; CKD-HP: P_i 0.9%; CKD-EP: P_i 1.2%; CKD-LaC: P_i 1.2% and 6% lanthanum carbonate. Diets in the CKD groups contained 0.3% adenine. Values are means ± SE. One-way ANOVA followed by a Tukey-Kramer test was performed. A 2-tailed $P < 0.05$ was considered statistically significant. *$P < 0.05$ vs. CNT.

RESULTS

Dietary P_i loading induces a short lifespan. To determine the effects of P_i loading and P_i binder use, rats were divided into the following six groups and given different amounts of P_i: CNT, CKD-LP, CKD-MP, CKD-HP, CKD-EP, and CKD-LaC. The content of each diet is shown in Table 1. Four rats in the CKD-EP group and two rats in the CKD-HP group died during the study period (8 wk). All rats in the other four groups survived. Log-rank tests revealed a significant difference in survival curves (Fig. 1*A*).

Dietary P_i loading induces aortic medial calcification. Figure 1*B* shows representative photomicrographs of the abdominal aorta stained using the von Kossa method. CKD-HP and CKD-EP rats developed moderate to severe degrees of aortic calcification, respectively; the other four groups did not. Aortic Ca^{2+} content increased in a dietary P_i loading-dependent fashion in CKD rats. Lanthanum carbonate lowered the Ca^{2+} content, which had increased with P_i loading (Fig. 1*C*).

Dietary P_i loading induces biochemical disorders in a concentration-dependent manner. Table 2 shows the findings of serum and urinary biochemical analyses after 8 wk. Dietary P_i loading increased the amount of urinary P_i excretion, serum levels of P_i, intact parathyroid hormone, and serum FGF_{23} in a dose-dependent manner. Lanthanum carbonate significantly attenuated these P_i-related changes. The serum Ca^{2+} level was dependent on the Ca^{2+}-to-P_i ratio in an inverse relationship with dietary P_i content. Serum levels of calcitriol in all CKD rats were significantly lower than those levels in CNT rats. Calcitriol levels in CKD rats were comparable among groups. Serum levels of fetuin-A were comparable among CKD rats (data not shown).

Dietary P_i loading does not influence systolic blood pressure level, kidney function, and urinary protein excretion. The effects of diets on systolic blood pressure, kidney histology, kidney function, and proteinuria were determined (Table 3 and Fig. 2). Systolic blood pressure levels were comparable among groups at each time point, ruling out the effects of different diets on blood pressure level and blood pressure-related vascular changes, including VC. Histological evaluation of the kidney by Masson trichrome staining revealed that tubulointerstitial fibrosis, cellular infiltration, and deposition of adenine crystals in renal tubules and the renal interstitium were present in all CKD groups, and Ca^{2+}-P_i deposition was observed only in CKD-HP and CKD-EP rats, reflecting the relatively high P_i burden on the kidneys in these two groups (Fig. 2*A*). However, the extent of tissue injury was almost comparable among the five CKD groups. In fact, serum Cr levels in all CKD rats were significantly higher than those levels in CNT rats, and Cr clearances in all CKD rats were significantly lower than in CNT rats, whereas there was no significant difference among the five CKD groups (Fig. 2, *B* and *C*). There was no statistical difference in urinary protein excretion among the six groups (Fig. 2*D*).

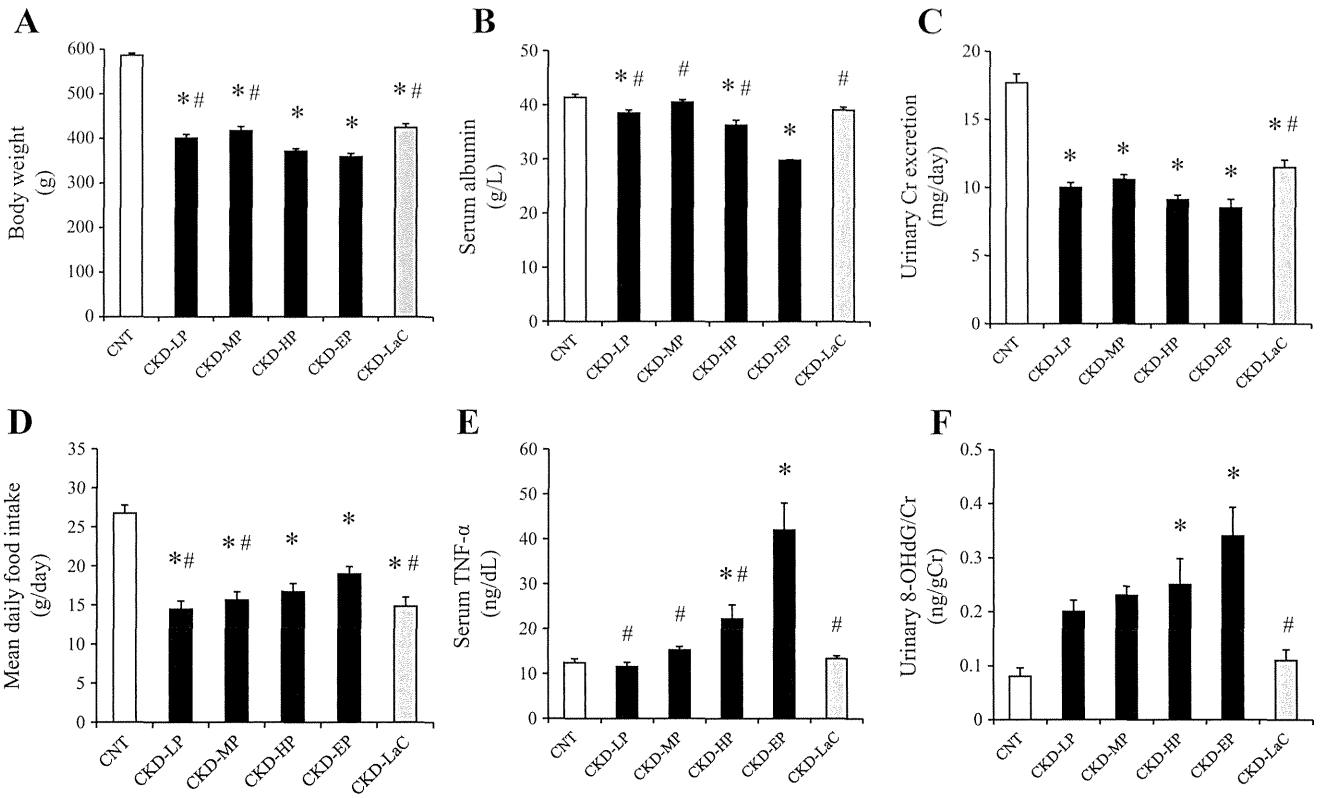

Fig. 3. Effects of dietary P_i loading on nutritional status and systemic inflammation and oxidative stress markers. *A*: body weight. *B*: serum albumin level. *C*: urinary Cr excretion. *D*: mean daily food intake. *E*: serum TNF-α level. *F*: urinary 8-hydroxy-2′-deoxyguanosine (8-OHdG)-to-Cr ratio (8-OHdG/Cr). Mean daily food intake was calculated using the arithmetic mean of food intake at *weeks 2*, *4*, *6*, and *8*. Data are expressed as means ± SE. One-way ANOVA followed by the Tukey-Kramer test was performed. Two-tailed *P* values of <0.05 were considered statistically significant. *$P < 0.05$ vs. the CNT group; #$P < 0.05$ vs. the CKD-EP group.

Dietary P_i loading induces malnutrition in a concentration-dependent manner. To determine the effects of dietary P_i loading on nutritional status, body weights and serum albumin levels were measured. Urinary Cr excretion was used as the surrogate marker for total muscle mass. Body weight, serum albumin, and urinary Cr excretion at *week 8* decreased in a P_i concentration-dependent manner. Lanthanum carbonate abrogated all changes related to dietary P_i overload (Fig. 3, *A–C*). Food intake in CKD-EP rats was significantly higher compared with CKD-LP, CKD-MP, and CKD-LaC rats (Fig. 3*D*), indicating that the decrease in body weight was not caused by reduced food intake.

Dietary P_i loading promotes systemic inflammation and oxidative stress. To determine the effects of P_i loading on systemic inflammation and oxidative stress, serum TNF-α and urinary 8-OHdG/Cr levels were measured. Dietary P_i loading increased serum TNF-α levels in CKD rats dose dependently. Lanthanum carbonate significantly inhibited the increase (Fig. 3*E*). Similarly, dietary P_i loading dose dependently increased urinary 8-OHdG/Cr levels in CKD rats, which was ameliorated by lanthanum carbonate (Fig. 3*F*).

The level of serum P_i is strongly correlated with the extent of MIA syndrome. To determine the association between derangement in P_i metabolism and MIA components, simple linear regression analysis was performed. The serum P_i level was significantly correlated with each MIA component, including serum TNF-α levels (Fig. 4, *A–F*). Furthermore, serum TNF-α was significantly correlated with MIA components (body weight, serum albumin, aortic Ca^{2+} content, and 8-OHdG/Cr; Fig. 5, *A–D*).

Multivariable analysis showed that the serum TNF-α level was significantly correlated with body weight, serum albumin level, urinary 8-OHdG level, and aortic Ca^{2+} content even after adjusting for Cr clearance, indicating that these associations were independent of kidney function [body weight ($r = -0.353$, $P < 0.05$), serum albumin ($r = -0.523$, $P < 0.05$), aortic Ca^{2+} content ($r = 0.405$, $P < 0.05$), and urinary 8-OHdG/Cr ($r = 0.663$, $P < 0.05$)].

P_i loading increases oxidative stress and inflammation in the kidney, heart, and aorta. To determine whether P_i loading induces local inflammation, relative mRNA levels of TNF-α in the aorta, heart, and kidney in the CNT, CKD-LP, CKD-EP, and CKD-LaC groups were examined. mRNA levels of TNF-α in the aorta, heart, and kidney of CKD-EP rats were significantly higher than those levels in CNT rats. The increases were significantly attenuated with low dietary P_i loading and lanthanum treatment (Fig. 6, *A–C*).

Next, to determine local oxidative stress levels, immunohistochemistry for 8-OHdG in the aorta was performed (Fig. 6*D*). The 8-OHdG-positive number in CKD-EP rats was significantly increased compared with CNT rats. The positive numbers in CKD-LP and CKD-LaC rats were lower than CKD-EP rats, a finding that was confirmed by semiquantitative analysis (Fig. 6*E*). Immunohistochemistry of the aorta for Ser^{276} phosphorylated p65 was also performed. Strong staining of phosphorylated p65 was observed only in the calcified area of CKD-EP rats (Fig. 6*F*). The positive areas in CKD-LP and CKD-LaC rats were lower than CKD-EP rats, a finding that was confirmed by semiquantitative analysis (Fig. 6*G*). These

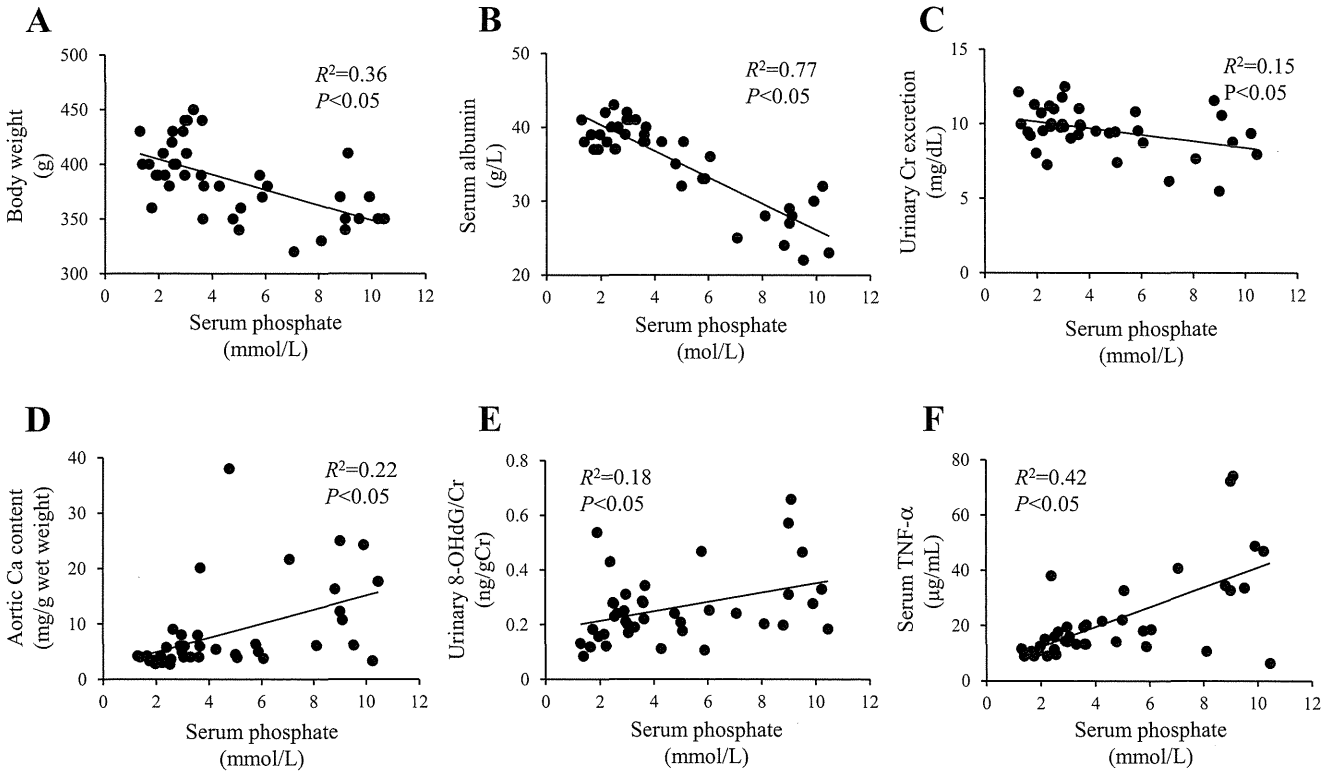

Fig. 4. Correlations between serum P_i and components of malnutrition-inflammation-atherosclerosis (MIA) syndrome. *A–F*: correlation of serum P_i with body weight (*A*), serum albumin (*B*), urinary Cr excretion (*C*), aortic Ca^{2+} content (*D*), urinary 8-OHdG/Cr (*E*), and serum TNF-α (*F*). The correlation coefficient (R^2) was determined using Pearson's method. Two-tailed *P* values of <0.05 were considered statistically significant.

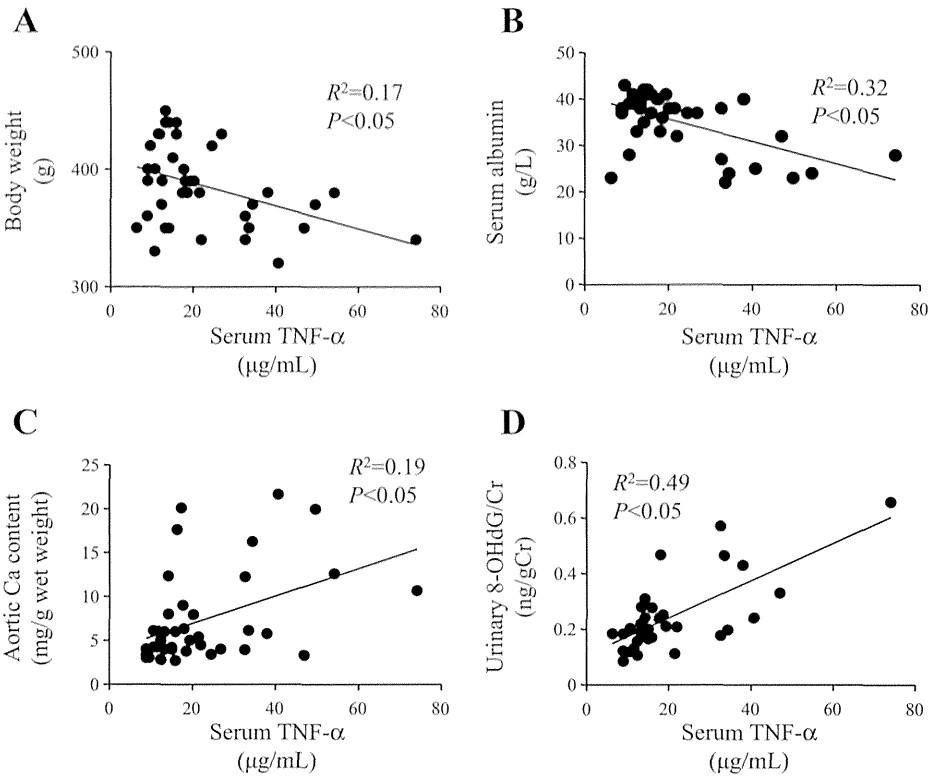

Fig. 5. Correlation between TNF-α and components of MIA syndrome. *A–D*: correlation of serum TNF-α with serum albumin (*A*), urinary Cr excretion (*B*), aortic Ca^{2+} content (*C*), and urinary 8-OHdG/Cr (*D*). R^2 values were determined using Pearson's method. Two-tailed P values of <0.05 were considered statistically significant.

results indicate that both inflammation and oxidative stress are activated in the calcified area of the aorta.

To determine the effect of P_i loading on the expression of Pit-1, the relative mRNA expression of Pit-1 in the aorta was examined. mRNA levels of Pit-1 in the aorta of CKD-EP rats were significantly higher than those levels in CNT rats. Additionally, the increase was significantly attenuated by low dietary P_i loading and lanthanum treatment (Fig. 6*H*).

P_i loading and uremia inhibit albumin and fetuin production in the rat liver. To determine the effects of P_i loading on negative acute-phase protein, mRNA levels of albumin and fetuin-A in the rat liver were determined. mRNA expression levels of albumin and fetuin-A significantly decreased in CKD-LP, CKD-EP, and CKD-LaC rats. The lowest level was observed in CKD-EP rats (Fig. 7, *A* and *B*). However, the difference in albumin and fetuin-A mRNA levels induced by P_i loading was relatively small compared with the effect of CKD.

P_i loading directly induces local inflammation in cultured HUASMCs but does not reduce negative acute-phase protein synthesis in HepG2 cells. To determine the direct effects of P_i loading on local inflammation, oxidative stress, and protein synthesis, an in vitro experiment using cultured HUASMCs and human HepG2 cells (a frequently used human liver hepatocytoma cell line for examining hepatocyte biology) was performed. High-P_i medium (2.9 mM) directly increased mRNA expression of TNF-α and Nox4 and decreased expression of Klotho in HUASMCs on *day 1* compared with normal-P_i medium (0.9 mM; Fig. 8, *A–C*). Bone morphogenetic protein-2 (a bone-related marker) did not increase at this time point, indicating that inflammation and oxidative stress precede the transdifferentiation of HUASMCs into osteoblast-like cells (Fig. 8*D*). High-P_i medium (2.9 mM) did not influence the synthesis of either albumin or fetuin-A in HepG2 cells compared with normal-P_i medium (0.9 mM) for 1 day (Fig. 8, *E* and *F*).

DISCUSSION

MIA syndrome is a prominent feature in CKD patients and contributes to increased mortality (41, 42, 48). Growing evidence has revealed the harmful effects of P_i overload on the cardiovascular system (4, 15, 23, 39, 43). However, the effects of P_i overload on the interactions among inflammation, malnutrition, and VC have not been investigated. To the best of our knowledge, the present study is the first to report that dietary P_i loading dose dependently induces inflammation and malnutrition as well as VC and premature death in uremic rats without affecting kidney function. Furthermore, use of a P_i binder and dietary P_i restriction almost reversed all of the P_i overload-related changes described above. These findings suggest that MIA syndrome is partially mediated by P_i overload in CKD and that appropriate management of P_i through dietary or pharmacological intervention or anti-inflammatory therapy may be a promising therapeutic strategy for the prevention of MIA syndrome in CKD.

Chronic inflammation is a common feature and a major cause of cardiovascular and other complications of CKD (50). Clinical studies have reported that serum P_i, Ca^{2+}-P_i product, and FGF_{23} correlate well with serum inflammatory markers in CKD patients (22, 28, 30). In the present study, P_i loading dose dependently induced inflammation in the aorta, heart, and kidneys and increased serum TNF-α levels in uremic rats. Linear regression analysis showed that there was a close association between P_i overload and serum TNF-α levels. Furthermore, in the present in vitro study, P_i overload directly increased the expression of TNF-α in VSMCs. Zhao et al. (53)

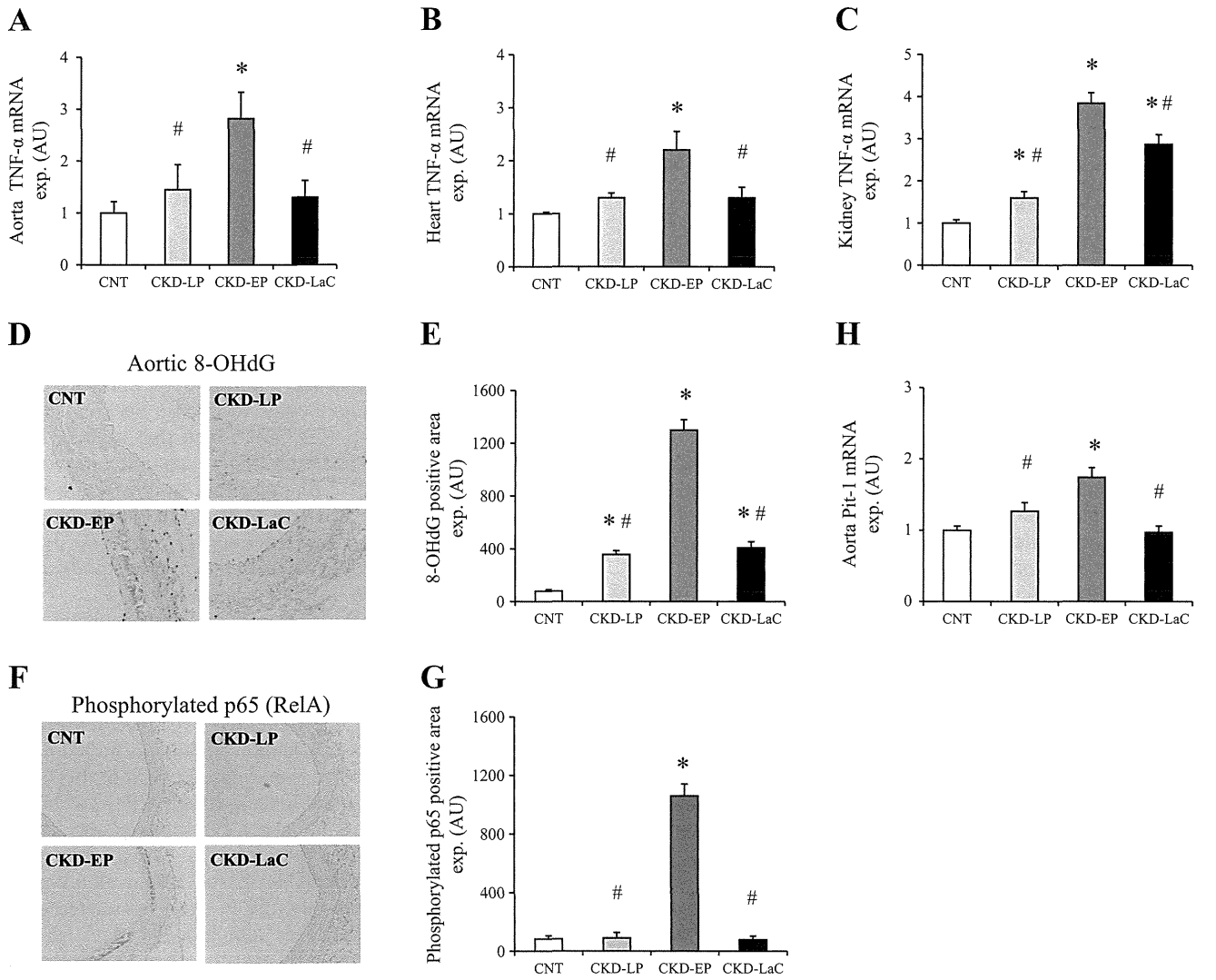

Fig. 6. Effects of P_i loading on local inflammation and oxidative stress levels. *A–C*: relative mRNA levels of tissue TNF-α in the rat aorta (*A*), heart (*B*), and kidney (*C*). *D*: representative microphotographs of immunohistochemistry for 8-OHdG in the aorta. Original magnification: ×200. *E*: quantification of the positively stained area for 8-OHdG in the aorta. *F*: representative microphotographs of immunohistochemistry for phosphorylated p65 (Ser^{276}, RelA) of the aorta. Original magnification: ×200). *G*: quantification of the positively stained area for phosphorylated p65 in the aorta. *H*: relative mRNA level of P_i transporter (Pit)-1 in the aorta. mRNA expression was corrected to the level of GAPDH. AU, arbitrary units. Data are expressed as means ± SE. One-way ANOVA followed by the Tukey-Kramer test was performed. Two-tailed *P* values of <0.05 were considered statistically significant. $*P < 0.05$ vs. the CNT group; $\#P < 0.05$ vs. the CKD-EP group.

reported that P_i loading induces the generation of mitochondrial ROS, leading to the activation of NF-κB signaling and VC in vivo and in vitro, an effect ameliorated by antioxidative drug treatment. In addition, TNF-α, which is induced by activation of the NF-κB pathway, in turn activates the NF-κB pathway (27). Collectively, these results strongly suggest that P_i loading directly induces local inflammation in uremia.

P_i inflow into the intracellular space by Pit-1 is one of the possible mechanisms of P_i-induced cellular inflammation. Recently, Voelkl et al. (47) reported that the expression of TNF-α was increased in the various tissues of Klotho knockout mice and that Pit-1 downregulation reversed the upregulation of TNF-α and calcification in VSMCs. P_i enters into cells via Pit-1, a Na^+-P_i co-transporter that is ubiquitously expressed in the cell membrane. This suggests that Pit-1 is critical for triggering P_i-induced local inflammation and the resulting VC in Klotho knockout mice. In the present study, cultured VSMCs exposed to P_i overload directly increased their mRNA expression of TNF-α and Nox4 (one of the NADPH oxidase family members), which occurred in parallel with decreases in Klotho mRNA, in advance of the increase in bone morphogenetic protein-2 (a marker of osteoblastic transdifferentiation). Furthermore, Pit-1 expression increased in aortas of CKD-EP rats. Collectively, the results of the present study suggest that P_i overload directly induces local inflammation and oxidative stress in a Pit-1-dependent manner and subsequently causes the adverse outcomes, including VC, in CKD.

Experimental studies have reported that oxidative stress and inflammation promote VC in CKD (10, 49, 53). An animal study (52) reported that inhibition of the NF-κB pathway ameliorated VC. Because both oxidative stress and inflammatory responses share the NF-κB pathway, and because phosphorylation of p65 indicates the activation of NF-κB signaling,

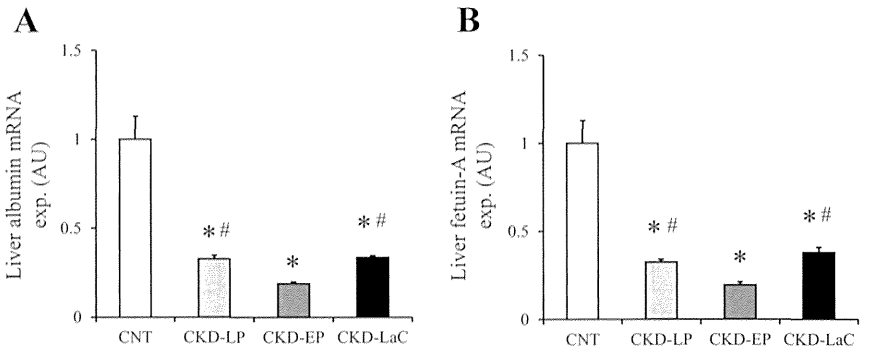

Fig. 7. Effects of P_i loading on the synthesis of albumin and fetuin-A in the rat liver. *A* and *B*: mRNA expression of albumin (*A*) and fetuin-A (*B*) in the rat liver. mRNA expression was corrected to the level of GAPDH. Data are expressed as means ± SE. One-way ANOVA followed by the Tukey-Kramer test was performed. Two-tailed *P* values of <0.05 were considered statistically significant. $*P < 0.05$ vs. the CNT group; $\#P < 0.05$ vs. the CKD-EP group.

the results of the present study are consistent with the hypothesis that aortic medial calcification is mediated by oxidative stress and inflammation in CKD (1, 52). Given the tight link between P_i loading and oxidative stress, the cross-talk between ROS and the NF-κB signaling pathway, and the important role of the NF-κB pathway in the pathogenesis of inflammation, inhibition of NF-κB signaling by antioxidant treatment has the potential to prevent the progression of P_i-induced MIA syndrome.

Another potential mechanism of P_i-induced inflammation other than the Pit-1 pathway should be considered because P_i entry through Pit-1 has been reported to be already saturated at physiological P_i concentrations (46), although upregulation of Pit-1 can increase the total P_i inflow into the intracellular space under high-P_i conditions. The fetuin-mineral complex (also called the calciprotein particle, matrix vesicle, or basic calcium phosphate crystal) is emerging as a substance that is thought to induce cardiovascular diseases (11, 14, 40). This is because the fetuin-mineral complex is formed extracellularly under high-P_i conditions, and the complex is incorporated into VSMCs via endocytosis and induces various type of responses that can promote VC, for example, apoptosis of VSMCs and a Ca^{2+} burst (34). Interestingly, VC was prevented by chelating the extracellular fetuin-mineral complex in an in vitro study of VSMCs exposed to high P_i. Furthermore, recent experimental studies have reported that the fetuin-mineral complex directly induces macrophages/monocytes to release an array of cytokines, including TNF-α (29, 32). Given that high P_i loading increases the levels of the fetuin-mineral complex in serum and tissue in an adenine-fed rat model (24), the fetuin-mineral complex may be a direct cause of local and systemic inflammation and malnutrition in uremic rats with P_i overload. Further studies are needed to clarify the precise pathogenesis of P_i-related inflammation and the progression of VC.

The mechanism of P_i overload-induced malnutrition is another important subject. In the present study, malnutrition may be partly explained by chronic inflammation and oxidative stress (7, 21). Proinflammatory cytokines (TNF-α, IL-1, and IL-6) are known to induce oxidative stress, decrease hepatic albumin synthesis, cause systemic catabolism (including muscle degradation), and increase energy expenditure, leading to a decrease in body weight and muscle atrophy (9, 33). Oxidative stress also produces inflammatory cytokines in the liver and muscle (8). Collectively, these results explain our present observation that P_i overload decreased serum albumin level, body weight, and muscle mass by P_i overload-related chronic inflammation. Furthermore, as albumin also acts as a very important serum antioxidant by exerting glutathion-linked thiol peroxidase activity (5), the reduction in serum albumin facili-

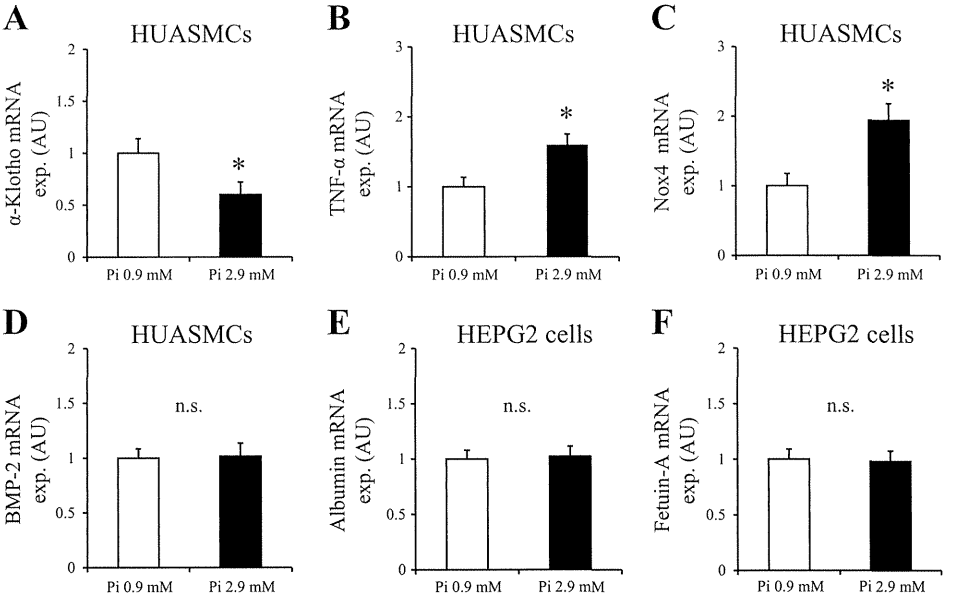

Fig. 8. Direct effects of P_i loading on the phenotype of human umbilical arterial smooth muscle cells (HUASMCs) and HepG2 cells. *A–F*: mRNA expression of α-Klotho (*A*), TNF-α (*B*), NADPH oxidase 4 (Nox4; *C*), and bone morphogenetic protein (BMP)-2 (*D*) in HUASMCs and albumin (*E*) and fetuin-A (*F*) in HepG2 cells. HUASMCs and HepG2 cells were exposed to culture media containing 0.9 or 2.9 mM P_i for 1 day. mRNA expression was corrected to the level of GAPDH. Data are expressed as means ± SE. An unpaired *t*-test was performed. Two-tailed *P* values of <0.05 were considered statistically significant. $*P < 0.05$ vs. 0.9 mM P_i.

tates oxidative stress and inflammation, leading to the vicious cycle between malnutrition and inflammation.

The P_i-induced decrease in the serum albumin level is another interesting issue. In the present study, both decreased kidney function and P_i loading might be equally involved in decreased albumin synthesis. With regard to decreased albumin synthesis, P_i-induced systemic inflammation might be possible, because P_i loading did not directly decrease albumin synthesis in HepG2 cells. Because the decrease in the serum albumin level was not proportional to the decrease in albumin synthesis in the rat liver, albumin degradation might be involved in the reduction in the serum albumin level; the serum albumin level is determined by the balance between albumin synthesis and albumin degradation. Experimental studies have shown that inflammation promotes albumin degradation through the neonatal Fc receptor pathway (6, 20, 45). These results indicate that P_i-induced inflammation could have also accelerated albumin degradation in the present in vivo study. Collectively, the P_i-induced reduction in the serum albumin level can be explained by both decreased albumin synthesis and enhanced albumin degradation. However, further studies are required to identify the precise mechanisms for how P_i overload induces hypoalbuminemia.

The effects of dietary P_i restriction and P_i binder use on inflammation and malnutrition were compared. Both dietary P_i restriction and P_i binder use equally decreased the levels of TNF-α and urinary 8-OHdG/Cr, ameliorated VC, and produced a survival advantage. These results indicate that the amount of P_i absorbed from the gut primarily determines the degree of MIA syndrome. In contrast, dietary P_i restriction is frequently accompanied by protein restriction (18), and clinical studies have suggested the potential harm of P_i restriction (36). However, no detrimental effects were observed in CKD-LP rats in the present study because P_i and protein restriction were successfully separated by providing synthetic diets. Given that P_i restriction inevitably induces protein restriction in clinical medicine, P_i binder use may be a more practical way of preventing P_i-related MIA syndrome in CKD patients.

There are several limitations in the present study. First, urinary P_i excretion in CNT rats was extremely decreased compared with the CKD-EP rats, although the P_i concentrations in these two groups were identical. This is because the food for CNT rats contained grain-based protein and did not contain 20% lactose; these differences in the diet directly affected the absorption rate of P_i from the intestine. Second, the level of food intake in each group was slightly different. However, the amount of food intake in rats fed the extremely high-P_i diet was greater than that observed in rats fed the low-P_i diet, indicating that malnutrition was not induced by decreased food intake but rather by P_i overload in the setting of CKD. Third, we observed an association among P_i loading, inflammation, and malnutrition but did not examine the putative cause-effect relationship by directly intervening in the inflammatory process related to P_i loading. We did not determine the precise mechanism for how P_i induces inflammation via Na^+-P_i cotransporters and/or via the formation and endocytosis of the P_i-related fetuin-mineral complex. However, taking into account these limitations, we believe that P_i overload induces inflammation and malnutrition as well as VC in subjects with CKD and that the present study sheds light on another important harmful effect of P_i overload on CKD status.

In conclusion, this study demonstrated that dietary P_i overload directly induces chronic inflammation and malnutrition as well as VC in CKD rats. These data suggest that chronic inflammation induced by P_i overload plays a pivotal role in the pathogenesis of MIA syndrome in CKD and that inhibition of P_i loading through dietary or pharmacological intervention or anti-inflammatory therapy may be a promising treatment for the prevention of MIA syndrome.

ACKNOWLEDGMENTS

The authors thank Noriko Noda and Mika Oonishi for clerical management of the study and Tomoe Fujino for technical support in the preparation and determination of the biochemical parameters. The authors also thank Edanz (http://www.edanzediting.co.jp/) for the English editing of the manuscript.

GRANTS

This work was partly supported by the Japanese Association of Dialysis Physicians and MEXT-Supported Program for the Strategic Research Foundation at Private Universities.

DISCLOSURES

No conflicts of interest, financial or otherwise, are declared by the author(s).

AUTHOR CONTRIBUTIONS

Author contributions: S.Y. conception and design of research; S.Y., M. Tokumoto, N.T., and H.N. performed experiments; S.Y., M. Tokumoto, and H.N. analyzed data; S.Y., M. Tokumoto, M. Taniguchi, T.N., and K.M. interpreted results of experiments; S.Y. prepared figures; S.Y., M. Tokumoto, H.O., and K.T. drafted manuscript; S.Y. edited and revised manuscript; S.Y., M. Tokumoto, N.T., M. Taniguchi, H.N., T.N., K.M., H.O., K.T., and T.K. approved final version of manuscript.

REFERENCES

1. **Al-Aly Z.** Phosphate, oxidative stress, and nuclear factor-κB activation in vascular calcification. *Kidney Int* 79: 1044–1047, 2011.
2. **Atkinson J.** Age-related medial elastocalcinosis in arteries: mechanisms, animal models, and physiological consequences. *J Appl Physiol* 105: 1643–1651, 2008.
3. **Barreto DV, Barreto FC, Liabeuf S, Temmar M, Lemke HD, Tribouilloy C, Choukroun G, Vanholder R, Massy ZA.** Plasma interleukin-6 is independently associated with mortality in both hemodialysis and pre-dialysis patients with chronic kidney disease. *Kidney Int* 77: 550–556, 2010.
4. **Block GA, Klassen PS, Lazarus JM, Ofsthun N, Lowrie EG, Chertow GM.** Mineral metabolism, mortality, and morbidity in maintenance hemodialysis. *J Am Soc Nephrol* 15: 2208–2218, 2004.
5. **Cha MK, Kim IH.** Glutathione-linked thiol peroxidase activity of human serum albumin: a possible antioxidant role of serum albumin in blood plasma. *Biochem Biophys Res Commun* 222: 619–625, 1996.
6. **Chaudhury C, Mehnaz S, Robinson JM, Hayton WL, Pearl DK, Roopenian DC, Anderson CL.** The major histocompatibility complex-related Fc receptor for IgG (FcRn) binds albumin and prolongs its lifespan. *J Exp Med* 197: 315–322, 2003.
7. **Darlington GJ, Wilson DR, Lachman LB.** Monocyte-conditioned medium, interleukin-1, and tumor necrosis factor stimulate the acute phase response in human hepatoma cells in vitro. *J Cell Biol* 103: 787–793, 1986.
8. **Dong W, Simeonova PP, Gallucci R, Matheson J, Fannin R, Montuschi P, Flood L, Luster MI.** Cytokine expression in hepatocytes: role of oxidant stress. *J Interferon Cytokine Res* 18: 629–638, 1998.
9. **Fleet M, Osman F, Komaragiri R, Fritz A, D.** Protein catabolism in advanced renal disease: role of cytokines. *Clin Nephrol* 70: 91–100, 2008.
10. **Guerrero F, Montes de Oca A, Aguilera-Tejero E, Zafra R, Rodríguez M, López I.** The effect of vitamin D derivatives on vascular calcification associated with inflammation. *Nephrol Dial Transplant* 27: 2206–2212, 2012.
11. **Hamano T, Matsui I, Mikami S, Tomida K, Fujii N, Imai E, Rakugi H, Isaka Y.** Fetuin-mineral complex reflects extraosseous calcification stress in CKD. *J Am Soc Nephrol* 21: 1998–2007, 2010.
12. **Hruska KA, Mathew S, Lund R, Qiu P, Pratt R.** Hyperphosphatemia of chronic kidney disease. *Kidney Int* 74: 148–157, 2008.

13. **Isakova T, Gutiérrez OM, Chang Y, Shah A, Tamez H, Smith K, Thadhani R, Wolf M.** Phosphate binders and survival on hemodialysis. *J Am Soc Nephrol* 20: 388–396, 2009.
14. **Jahnen-Dechent W, Heiss A, Schäfer C, Ketteler M.** Fetuin-A regulation of calcified matrix metabolism. *Circ Res* 108: 1494–1509, 2011.
15. **Jono S, McKee MD, Murry CE, Shioi A, Nishizawa Y, Mori K, Morii H, Giachelli CM.** Phosphate regulation of vascular smooth muscle cell calcification. *Circ Res* 87: E10–E17, 2000.
16. **Kakuta T, Tanaka R, Hyodo T, Suzuki H, Kanai G, Nagaoka M, Takahashi H, Hirawa N, Oogushi Y, Miyata T, Kobayashi H, Fukagawa M, Saito A.** Effect of sevelamer and calcium-based phosphate binders on coronary artery calcification and accumulation of circulating advanced glycation end products in hemodialysis patients. *Am J Kidney Dis* 57: 422–431, 2011.
17. **Kalantar-Zadeh-K, Ikizler TA, Block G, Avram MM, Kopple JD.** Malnutrition-Inflammation complex syndrome in dialysis patients: causes and consequences. *Am J Kidney Dis* 42: 864–881, 2003.
18. **Kalantar-Zadeh K, Gutekunst L, Mehrotra R, Kovesdy CP, Bross R, Shinaberger CS, Noori N, Hirschberg R, Benner D, Nissenson AR, Kopple JD.** Understanding sources of dietary phosphorus in the treatment of patients with chronic kidney disease. *Clin J Am Soc Nephrol* 5: 519–530, 2010.
19. **Kawata T, Nagano N, Obi M, Miyata S, Koyama C, Kobayashi N, Wakita S, Wada M.** Cinacalcet suppresses calcification of the aorta and heart in uremic rats. *Kidney Int* 74: 1270–1277, 2008.
20. **Kim J, Bronson CL, Hayton WL, Radmacher MD, Roopenian DC, Robinson JM, Anderson CL.** Albumin turnover: FcRn-mediated recycling saves as much albumin from degradation as the liver produces. *Am J Physiol Gastrointest Liver Physiol* 290: G352–G360, 2006.
21. **Kotur-Stevuljevic J, Simic-Ogrizovic S, Dopsaj V, Stefanovic A, Vujovic A, Ivanic-Corlomanovic T, Spasic S, Kalimanovska-Spasojevic V, Jelic-Ivanovic Z.** A hazardous link between malnutrition, inflammation and oxidative stress in renal patients. *Clin Biochem* 45: 1202–1205, 2012.
22. **Lee CT, Tsai YC, Ng HY, Su Y, Lee WC, Lee LC, Chiou TT, Liao SC, Hsu KT.** Association between C-reactive protein and biomarkers of bone and mineral metabolism in chronic hemodialysis patients: a cross-sectional study. *J Ren Nutr* 19: 220–227, 2009.
23. **London GM, Guerin AP, Marchais SJ, Metivier F, Pannier B, Adda H.** Arterial media calcification in end-stage renal disease: impact on all-cause and cardiovascular mortality. *Nephrol Dial Transplant* 18: 1731–1740, 2003.
24. **Matsui I, Hamano T, Mikami S, Fujii N, Takabatake Y, Nagasawa Y, Kawada N, Ito T, Rakugi H, Imai E, Isaka Y.** Fully phosphorylated fetuin-A forms a mineral complex in the serum of rats with adenine-induced renal failure. *Kidney Int* 75: 915–928, 2009.
25. **Mitch WE.** Insight into the abnormalities of chronic renal disease attributed to malnutrition. *J Am Soc Nephrol* 13, *Suppl* 1: S22–S27, 2002.
26. **Moe SM, Chen NX, Seifert MF, Sinders RM, Duan D, Chen X, Liang Y, Radcliff JS, White KE, Gattone VH 2nd.** A rat model of chronic kidney disease-mineral bone disorder. *Kidney Int* 75: 176–184, 2009.
27. **Morgan MJ, Liu ZG.** Crosstalk of reactive oxygen species and NF-κB signaling. *Cell Res* 21: 103–115, 2011.
28. **Munoz Mendoza J, Isakova T, Ricardo AC, Xie H, Navaneethan SD, Anderson AH, Bazzano LA, Xie D, Kretzler M, Nessel L, Hamm LL, Negrea L, Leonard MB, Raj D, Wolf M.** Fibroblast growth factor 23 and inflammation in CKD. *Clin J Am Soc Nephrol* 7: 1156–1162, 2012.
29. **Nadra I, Mason JC, Philippidis P, Florey O, Smythe CD, McCarthy GM, Landis RC, Haskard DO.** Proinflammatory activation of macrophages by basic calcium phosphate crystals via protein kinase C and MAP kinase pathways: a vicious cycle of inflammation and arterial calcification? *Circ Res* 96: 1248–1256, 2005.
30. **Navarro-González JF, Mora-Fernádez C, Muros de Fuentes M, Herrera H, Garcia J.** Mineral metabolism and inflammation in chronic kidney disease patients: a cross-sectional study. *Clin J Am Soc Nephrol* 4: 1646–1654, 2009.
31. **Neven E, Dams G, Postnov A, Chen B, De Clerck N, De Broe ME, D'Haese PC, Persy V.** Adequate phosphate binding with lanthanum carbonate attenuates arterial calcification in chronic renal failure rats. *Nephrol Dial Transplant* 24: 1790–1799, 2009.
32. **Pazár BP, Ea HK, Narayan S, Kolly L, Bagnoud N, Chobaz V, Roger T, Lioté F, So A, Busso N.** Basic calcium phosphate crystals induce monocyte/macrophage IL-1β secretion through the NLRP3 inflammasome in vitro. *J Immunol* 186: 2495–2502, 2011.
33. **Raj DS, Moseley P, Dominic EA, Onime A, Tzamaloukas AH, Boyd A, Shah VO, Glew R, Wolfe R, Ferrando A.** Interleukin-6 modulates hepatic and muscle protein synthesis during hemodialysis. *Kidney Int* 73: 1054–1061, 2008.
34. **Sage AP, Lu J, Tintut Y, Demer LL.** Hyperphosphatemia-induced nanocrystals upregulate the expression of bone morphogenetic protein-2 and osteopontin genes in mouse smooth muscle cells in vitro. *Kidney Int* 79: 414–422, 2011.
35. **Shanahan CM, Crouthamel MH, Kapustin A, Giachelli CM.** Arterial calcification in chronic kidney disease: key roles of calcium and phosphate. *Circ Res* 109: 697–711, 2011.
36. **Shinaberger CS, Greenland S, Kopple JD, Van Wyck D, Mehrotra R, Kovesdy CP, Kalantar-Zadeh K.** Is controlling phosphorus by decreasing dietary protein intake beneficial or harmful in persons with chronic kidney disease? *Am J Clin Nutr* 88: 1511–1518, 2008.
37. **Shlipak MG, Fried LF, Crump C, Bleyer AJ, Manolio TA, Tracy RP, Furberg CD, Psaty BM.** Elevations of inflammatory and procoagulant biomarkers in elderly persons with renal insufficiency. *Circulation* 107: 87–92, 2003.
38. **Shobeiri N, Adams MA, Holden RM.** Vascular calcification in animal models of CKD: a review. *Am J Nephrol* 31: 471–481, 2010.
39. **Shuto E, Taketani Y, Tanaka R, Harada N, Isshiki M, Sato M, Nashiki K, Amo K, Yamamoto H, Higashi Y, Nakaya Y, Takeda E.** Dietary phosphorus acutely impairs endothelial function. *J Am Soc Nephrol* 20: 1504–1512, 2009.
40. **Smith ER, Ford ML, Tomlinson LA, Rajkumar C, McMahon LP, Holt SG.** Phosphorylated fetuin-A-containing calciprotein particles are associated with aortic stiffness and a procalcific milieu in patients with pre-dialysis CKD. *Nephrol Dial Transplant* 27: 1957–1966, 2012.
41. **Stenvinkel P, Heimburger O, Paultre F, Diczfalusy U, Wang T, Berglund L, Jogestrand T.** Strong association between malnutrition, inflammation, and atherosclerosis in chronic renal failure. *Kidney Int* 55: 1899–1911, 1999.
42. **Stenvinkel P, Heimburger O, Lindholm B, Kaysen GA, Bergstrom J.** Are there two types of malnutrition in chronic renal failure? Evidence for relationships between malnutrition, inflammation and atherosclerosis (MIA syndrome). *Nephrol Dial Transplant* 15: 953–960, 2000.
43. **Son BK, Kozaki K, Iijima K, Eto M, Kojima T, Ota H, Senda Y, Maemura K, Nakano T, Akishita M, Ouchi Y.** Statins protect human aortic smooth muscle cells from inorganic phosphate-induced calcification by restoring Ga6-Axl survival pathway. *Circ Res* 98: 1024–1031, 2006.
44. **Takeda E, Taketani Y, Morita K, Tatsumi S, Katai K, Nii T, Yamamoto H, Miyamoto K.** Molecular mechanisms of mammalian inorganic phosphate homeostasis. *Adv Enzyme Regul* 40: 285–302, 2000.
45. **van Bilsen K, van Hagen PM, Bastiaans J, van Meurs JC, Missotten T, Kuijpers RW, Hooijkaas H, Dingjan GM, Baarsma GS, Dik WA.** The neonatal Fc receptor is expressed by human retinal pigment epithelial cells and is downregulated by tumour necrosis factor-α. *Br J Ophthalmol* 95: 864–868, 2011.
46. **Villa-Bellosta R, Bogaert YE, Levi M, Sorribas V.** Characterization of phosphate transport in rat vascular smooth muscle cells: implications for vascular calcification. *Arterioscler Thromb Vasc Biol* 27: 1030–1036, 2007.
47. **Voelkl J, Alesutan I, Leibrock CB, Quintanilla-Martinez L, Kuhn V, Feger M, Mia S, Ahmed MS, Rosenblatt KP, Kuro-OM, Lang F.** Spironolactone ameliorates PIT1-dependent vascular osteoinduction in klotho-hypomorphic mice. *J Clin Invest* 123: 812–822, 2013.
48. **Wang AY, Woo J, Lam CW, Wang M, Chan IH, Gao P, Lui SF, Li PK, Sanderson JE.** Associations of serum fetuin-A with malnutrition, inflammation, atherosclerosis and valvular calcification syndrome and outcome in peritoneal dialysis patients. *Nephrol Dial Transplant* 20: 1676–1685, 2005.
49. **Yamada S, Taniguchi M, Tokumoto M, Toyonaga J, Fujisaki K, Suehiro T, Noguchi H, Iida M, Tsuruya K, Kitazono T.** The antioxidant tempol ameliorates arterial medial calcification in uremic rats: important role of oxidative stress in the pathogenesis of vascular calcification in chronic kidney disease. *J Bone Miner Res* 27: 474–485, 2012.
50. **Yeun JY, Levine RA, Mantadilok V, Kaysen GA.** C-reactive protein predicts all-cause and cardiovascular mortality in hemodialysis patients. *Am J Kidney Dis* 35: 469–476, 2000.
51. **Yokozawa T, Zheng PD, Oura H, Koizumi F.** Animal model of adenine-induced chronic renal failure in rats. *Nephron* 44: 230–234, 1986.
52. **Zhao G, Xu MJ, Zhao MM, Dai XY, Kong W, Wilson GM, Guan Y, Wang CY, Wang X.** Activation of nuclear factor-κB accelerates vascular calcification by inhibiting ankylosis protein homolog expression. *Kidney Int* 82: 34–44, 2012.
53. **Zhao MM, Xu MJ, Cai Y, Zhao G, Guan Y, Kong W, Tang C, Wang X.** Mitochondrial reactive oxygen species promote p65 nuclear translocation mediating high-phosphate-induced vascular calcification in vitro and in vivo. *Kidney Int* 79: 1071–1079, 2011.

Life Sciences 113 (2014) 55–59

Contents lists available at ScienceDirect

Life Sciences

journal homepage: www.elsevier.com/locate/lifescie

Improvement in spatial memory dysfunction by telmisartan through reduction of brain angiotensin II and oxidative stress in experimental uremic mice

Naoki Haruyama [a], Kiichiro Fujisaki [a], Mayumi Yamato [b], Masahiro Eriguchi [a], Hideko Noguchi [a], Kumiko Torisu [a], Kazuhiko Tsuruya [a,c,*], Takanari Kitazono [a]

[a] Department of Medicine and Clinical Science, Graduate School of Medical Sciences, Kyushu University, Fukuoka, Japan
[b] Department of REDOX Medicinal Science, Faculty of Pharmaceutical Sciences, Kyushu University, Fukuoka, Japan
[c] Department of Integrated Therapy for Chronic Kidney Disease, Graduate School of Medical Sciences, Kyushu University, Fukuoka, Japan

ARTICLE INFO

Article history:
Received 23 February 2014
Accepted 23 July 2014
Available online 10 August 2014

Chemical compounds studied in this article:
Angiotensin II (PubChem CID: 172198)
8-oxo-hydroxydeoxyguanosine (PubChem CID: 73318)
Florisil (PubChem CID: 61680)
Malondialdehyde (PubChem CID: 10964)
Telmisartan (PubChem CID: 65999)
2-thiobarbituric acid (PubChem CID: 2723628)

Keywords:
Brain angiotensin II
Chronic kidney disease
Cognitive impairment
Oxidative stress
Telmisartan

ABSTRACT

Aims: We previously reported that chronic uremia induces spatial working memory dysfunction in mice, and that it is attributed to cerebral oxidative stress. The source of oxidative stress was considered to be uremic toxins, but this remains unclear. In the present study, we examined whether the brain renin–angiotensin system was activated in the CKD mouse model, and whether it contributed to cognitive impairment.

Main methods: CKD was induced in 8-week-old male mice by 5/6 nephrectomy. Mice were divided into four groups: control mice administered tap water (Cont-V), control mice treated with 0.5 mg/kg/day telmisartan, an angiotensin II (AII) receptor blocker, for 8 weeks (Cont-T), CKD mice administered tap water (CKD-V), and CKD mice treated with 0.5 mg/kg/day telmisartan for 8 weeks (CKD-T). After the treatment period, a radial arm water maze (RAWM) test was performed, and angiotensin II (AII) concentrations and markers of oxidative stress were measured in the brains of mice.

Key findings: Errors in the RAWM test were more frequent in the CKD-V group than in the Cont-V group. In addition, errors in the CKD-T group were comparable to control mice. Tissue brain AII concentrations were greater in the CKD-V group compared with the other groups. Oxidative DNA damage and lipid peroxidation in the brain were also greater in the CKD-V group compared with the other groups.

Significance: Our results suggest that brain AII levels were exaggerated in CKD mice, and that this contributes to cognitive impairment through oxidative stress.

Introduction

Chronic kidney disease (CKD) is a growing global health problem, having a prevalence of 10–16% in Asia, Europe, and the United States, and with elderly patients showing the highest incidence (Wen et al., 2008; Hallan et al., 2006; Coresh et al., 2007). Decreased glomerular filtration is independently correlated with all-cause mortality, cardiovascular diseases, and other comorbid diseases (Matsushita et al., 2010).

In addition to the diverse comorbidity of CKD, many clinical trials have confirmed the independent association between cognitive impairment and CKD (Khatri et al., 2009; Elias et al., 2009; Etgen et al., 2009). Researchers exploring the nature of cognition in CKD speculated that a number of potential causes related to CKD, such as oxidative stress, local inflammation, and the renin–angiotensin system (RAS), are attributed to the association (Madero et al., 2008; Bugnicourt et al., 2013).

Cognitive symptoms are typical manifestations of uremic encephalopathy. Researchers reported that accumulated uremic toxins (i.e., guanidino compounds and parathyroid hormone) induced excitatory neurological damage in patients with uremia (De Deyn et al., 2009). However, dialysis modalities and pharmacological intervention against secondary hyperparathyroidism are not likely to be effective at preventing the progression of cognitive impairment (Kurella-Tamura et al., 2013). Other factors, like neuro-endocrinal factors, may affect the pathophysiology of cognitive impairment in chronic dialysis patients, but this remains to be confirmed.

We recently reported that brain oxidative stress has a major role in spatial working memory dysfunction in a mouse model of chronic

* Corresponding author at: Department of Integrated Therapy for Chronic Kidney Disease, Graduate School of Medical Sciences, Kyushu University. 3-1-1 Maidashi, Higashi-ku, Fukuoka 812–8582, Japan. Tel.: +81 92 642 5843; fax: +81 92 642 5846.
E-mail address: tsuruya@intmed2.med.kyushu-u.ac.jp (K. Tsuruya).

http://dx.doi.org/10.1016/j.lfs.2014.07.032
0024-3205/

uremia (Fujisaki et al., 2014). In that study, treatment with an antioxidant, tempol, readily prevented memory dysfunction and neuronal damage of the hippocampus in mice. The essential cause of brain oxidative stress was considered to be uremic toxins, but the exact mechanism for the generation of oxidative stress was not determined.

In salt-induced hypertensive rats and chronic cerebral ischemia models, brain RAS was reported as a risk factor for oxidative stress in the brain and for cognitive dysfunction, which were prevented by RAS inhibition (beyond its blood pressure-lowering effect) (Pelisch et al., 2011; Inaba et al., 2009; Mogi et al., 2006; Tota et al., 2012). Recently, several reports suggest that uremic toxin may activate RAS. Shimizu et al. (2013) reported that indoxyl sulfate, a uremic toxin, induced expression of angiotensinogen via phosphorylation of CREB and activation of NF-kappa B in human renal tubular cells. Additionally, NF-kappa B could bind to a promoter region which regulates the activity of angiotensinogen in human renal tubular cells (Acres et al., 2011). These findings indicated that RAS could possibly be activated by certain uremic toxin. Therefore, we hypothesized that local brain RAS was one of the causative agents for accelerated cognitive dysfunction in CKD; and that telmisartan, the blocker of angiotensin II (AII) receptor, could prevent the local secretion of brain AII, leading to suppression of oxidative stress and improvement in memory dysfunction. To clarify these hypotheses, we used a uremic mouse model to examine the effects of telmisartan on cognitive dysfunction in CKD mice.

Materials and methods

Preparation of mice

Adult male C57BL/6 J mice were purchased from Nihon CLEA Corporation (Tokyo, Japan) and maintained on a 12-h light/dark cycle at 24 ± 1 °C and 40–70% relative humidity with free access to food and water at our facility. Eight-week-old mice were randomly divided into two groups: (1) the CKD group; and (2) the control group. Chronic renal failure was induced in mice in the CKD group using unilateral nephrectomy and 2/3 electrocoagulation of the contralateral renal cortex under anesthetization with inhaled induction of sevoflurane and an injection of pentobarbital (40 mg/kg body weight i.p.). Surgery was performed on 43 mice, with four of them dying within a few days after the operation. Sham operations were performed on control group mice. The following day, mice were further divided into groups: (1) control mice with orally administered vehicle (Cont-V, $n = 18$); (2) control mice treated with telmisartan (Cont-T, $n = 19$); (3) CKD mice orally administered vehicle (CKD-V, $n = 20$); and (4) CKD mice treated with telmisartan (CKD-T, $n = 19$). Telmisartan was dissolved in 1 mL of 1 N sodium hydroxide and neutralized by 1 N hydrochloric acid (HCl), then administered for 8 weeks at 0.5 mg/kg/day in drinking water. Blood pressure was measured using the indirect tail-cuff method with a blood pressure monitor (MK-2000; Muromachi Kikai Co., Tokyo, Japan), as described previously (Fujisaki et al., 2014).

All experimental procedures were conducted with the approval of the ethics committee for animal research at Kyushu University (#A24-167-2). The number of mice used and animal suffering were minimized in accordance with the Declaration of Helsinki.

Radial arm water maze (RAWM) test for spatial working memory assessment

To evaluate spatial working memory, the RAWM test was performed 8 weeks after the operation, as per the study of Fujisaki et al. Briefly, the water maze consisted of a circular tank 1 m in diameter. A clear circular platform was placed at the edge of the wall and submerged so that the top was just above the water surface. An electric lamp was placed outside the maze as a visual spatial cue. The maze was sectioned into six equal arms (each 19 cm wide), which radiated out from an open central area. The platform was moved at random to different corners of the arms each day. A mouse would swim from a randomly selected corner of the other five arms in each trial. Trials consisted of four acquisition trials (T1–T4) and one memory retention trial (T5). Each mouse was permitted to view the location of the platform for 1 min for each acquisition trial. After four acquisition trials, the mouse was kept in a cage for 30 min, before being made to swim for 1 min from the same corner as in the fourth trial (the memory retention trial). "Error" was defined as either: (1) the mouse went into the non-goal arm; or (2) the mouse did not reach the platform after entering the goal arm. For each error, the mouse was returned to the starting corner and the trial resumed. In the final trial on the last day, the number of errors in the RAWM test was counted.

Measurement of plasma and brain AII

AII levels of the brain cortex containing the hippocampus and blood plasma were examined. Mice were anesthetized with inhaled diethyl ether before blood was collected using the retro-orbital bleeding technique. Following transcardial perfusion with 20 mL saline, the brain was removed, and both cortex and hippocampus were dissected from the sample. For brain AII measurements, ipsilateral brain samples were homogenized in 1 mL of 0.1 N HCl and centrifuged at 10,000 × *g* at 4 °C for 30 min. The supernatant was used for radioimmunoassay of AII levels as described previously (Omata et al., 1996). First, for extraction of AII, Florisil adsorption and elution with acetone-HCl solution were used. Briefly, 300 μL of sample was mixed with 700 μL of Tris buffer (pH 8.6) and 30 mg of Florisil for 10 min. After centrifugation at 3,500 × *g* at 4 °C for 5 min, the supernatant was discarded, and the pellet was washed with distilled water twice. Then, the pellet was mixed with 250 μL of 0.5 N HCl and 750 μL of acetone for 10 min, and centrifuged at 3,500 × *g* at 4 °C for 5 min. The elution process was repeated twice. The supernatant was discarded and dried under a N_2 stream at 45 °C. Then, the sample was dissolved in Tris buffer contained EDTA-2Na and Tween-20 (pH 8.6). Next, for radioimmunoassay, 100 μL of extract was incubated with 100 μL of antibody solution (anti-AII rabbit serum) overnight at 4 °C. Iodinated AII (^{125}I-Angiotensin II) was added the following day and incubated overnight at 4 °C. On the 3rd day, 100 μL of anti-rabbit IgG goat serum as the second antibody and 100 μL of 25% polyethylene glycol solution were added, and the mixture was incubated for 1 h at 4 °C. After centrifugation at 3,500 × *g* at 4 °C for 20 min, the radioactivity of the pellet was determined using a gamma-counter. Concentrations were calculated using a standard curve. Results are expressed as femtomoles (fmol) per gram of tissue. The cross-reactivity of angiotensin I and angiotensin III for anti-AII rabbit serum is reported to be 0.035% and 21%, respectively, and the minimum measurable concentration is 0.96 fmol/mL (Omata et al., 1996). Blood plasma was extracted by centrifugation of the collected blood in a BD Microtainer tube (#365973; BD Diagnostics, Franklin Lakes, NJ) at 3,500 × *g* at 4 °C for 15 min and AII was measured using the same method mentioned above.

Immunohistochemistry for oxidative stress markers in the brain

We examined oxidative DNA damage in the CA3 sub-region of hippocampi by immunohistochemistry. Mice were perfused with 20 mL of 4% paraformaldehyde in phosphate buffered saline (PBS), pH 7.4. After the brain was removed, it was fixed with 10% formaldehyde for 24 h at room temperature. The sample was cut on a tissue slicer (MK-MC-01; Muromachi Kikai Co., Tokyo, Japan) and dehydrated in ethanol. Sections were then transferred to 1:1 (v/v) ethanol-xylene, cleared in toluene and embedded in Paraplast (Fisher Scientific, Pittsburgh, PA). The embedded sections were cut (4 μm thick) and mounted on glass slides. For immunohistochemistry, the sections were deparaffinized with xylene, dehydrated with ethanol and washed with distilled water. For antigen retrieval, the sections were digested by 0.1% proteinase K (Wako Pure Chemical Industries Ltd., Osaka, Japan)

for 15 min. To detect 8-hydroxy-2'-deoxyguanosine (8-OHdG) in nuclear DNA, the sections were pretreated with RNase A (10 mg/mL; Sigma-Aldrich, St Louis, MO) for 1 h and with 2 N HCl for 30 min. They were then blocked with 5% skim-milk in PBS for 30 min at room temperature. The sections were incubated at 4 °C overnight with 1 μg/mL of mouse monoclonal primary antibodies (clone N45.1; JaICA, Fukuroi, Japan) diluted in 0.2% Triton X-100/PBS. For endogenous peroxidase blocking, sections were incubated with 0.3% hydrogen peroxide diluted in methanol for 30 min. After several washes with 0.2% Triton X-100/PBS, sections were incubated with secondary antibodies (HRP conjugated goat anti-mouse (Fab') IgG, Nichirei Bioscientific Inc., Tokyo, Japan) for 30 min at room temperature. They were then incubated with 0.02% 3,3'-diaminobenzidine tetrahydrochloride (Nichirei) for ~5 min. Reactions were allowed to develop until judged sufficient using a light microscope. The intensity of 8-OHdG immunoreactivity in the section of the hippocampus was measured in each digital image using Image J 1.43 imaging software (National Institute of Mental Health, Bethesda, MD).

Determination of malondialdehyde

Malondialdehyde levels were determined using a thiobarbituric acid reactive substances assay kit (Northwest Life Science Specialties, Vancouver, Canada). The thiobarbituric acid reactive substances assay is generally used for estimation of lipid peroxidation and peroxidative tissue injury, which are reliable indices for indirect analyses of oxidative stress. Protein samples were obtained by homogenizing brain tissue with phosphate buffer (pH 7.0) and EDTA, and concentrations were determined using bicinchoninic acid protein assay reagent (Thermo Scientific, Waltham, MA) according to the manufacturer's protocol. Briefly, samples were mixed on ice with 10 μL butylated hydroxytoluene, 1 M phosphoric acid, and 250 μL 2-thiobarbituric acid. After vortex vigorously for 5 s, the reaction mixture was incubated for 60 min at 60 °C and centrifuged at 10,000 × *g* for 3 min. The supernatant was read at 532 nm. The signal was analyzed using a malondialdehyde standard curve. Results are expressed as nmol per mg protein.

Statistical analysis

All values are expressed as mean ± standard error of the mean (SEM). Statistical significance was assessed using one-way analysis of variance. A P value of <0.05 was considered statistically significant.

Results

Blood laboratory findings and group characteristics

Table 1 shows the characteristics of the four groups after evaluating for spatial memory function. In the CKD-V group, systolic blood pressure was significantly higher than that in the Cont-V group. Administration of telmisartan did not influence blood pressure in the CKD-T and Cont-T groups. Body weight and the degree of anemia were significantly lower in the CKD-V group compared with the Cont-V group. Administration of telmisartan did not change these values. For renal dysfunction, there was no significant difference between the CKD-V and CKD-T groups. Plasma AII was measured in all groups and was found to have increased in the CKD-T and Cont-T groups. Plasma AII of the CKD-V group had a tendency to be higher than that of the Cont-V group, but it was not significant.

Increase in AII concentrations in the brain of CKD mice and prevention by telmisartan

Brain AII concentrations in the CKD-V group were greater than in the Cont-V group (CKD-V: 161.2 ± 53.6; Cont-V: 88.2 ± 26.7 fmol/g of tissue in each group). Increases in brain AII concentrations in the CKD-V group were prevented with administration of telmisartan (CKD-T: 109.1 ± 10.5 fmol/g of tissue) (Fig. 1). This result was inconsistent with data of plasma angiotensin II concentrations from each group.

Accumulation of 8-OHdG in the hippocampus of CKD mice and prevention by telmisartan

The CA3 sub-region of the hippocampus in the CKD-V group exhibited stronger 8-OHdG immunoreactivity than that of the Cont-V group. In addition, telmisartan prevented its accumulation in both the CKD-T and Cont-T groups (Fig. 2).

Increase in malondialdehyde concentrations in the brain of CKD mice and prevention by telmisartan

The concentration of malondialdehyde was greater in the CKD-V group compared with the Cont-V group (CKD-V: 3.1 ± 0.4; Cont-V: 1.9 ± 0.4 nmol/mg protein, $n = 8$ in each group). Similar to brain AII concentrations, increases in malondialdehyde concentrations were less in the CKD-T group compared with the CKD-V group (1.3 ± 0.3 nmol/mg protein, $n = 8$) (Fig. 3).

Increase in errors in the RAWM test in CKD mice and prevention by telmisartan

Errors recorded for the RAWM test on the final day of trials (day 5) were greater in the CKD-V group than in the Cont-V group (3.9 ± 0.6 *vs.* 1.8 ± 0.6, respectively). The number of errors in the CKD-T group was comparable to the control groups (1.9 ± 0.4) (Fig. 4).

Discussion

The results of this study suggest that brain RAS was activated in CKD mice, and that inhibition of brain RAS contributed to the improvement in spatial working memory through attenuation of oxidative stress. These phenomena were independent of blood pressure or the degree of anemia.

It is well known that RAS components have various roles in the brain. For example, brain RAS maintains thirst, fluid metabolism, and sympathetic nerve activation in the subfornical organ and the hypothalamic paraventricular nucleus (Wilson et al., 2005; Huang and Johns, 2001; Dupont and Brouwers, 2010). A recent experimental study has shown that cognitive function is also affected by brain RAS (Dong et al., 2011). Brain renin is reported to be produced by neurons, and brain angiotensinogen mRNA was mainly observed in glial cells (Lavoie et al., 2004; Saavedra, 1992; Unger et al., 1988). Pelisch et al.

Table 1
Characteristics of the four groups after RAWM test.

Groups	Body weight (g)	SBP (mmHg)	Hematocrit (%)	Serum creatinine (mg/dL)	BUN (mg/dL)	Plasma AII (fmol/mL)
Cont-V ($n = 8$)	25.9 ± 0.6	120 ± 2	47.1 ± 0.8	0.12 ± 0.01	25 ± 2	12.8 ± 4.8
Cont-T ($n = 8$)	26.7 ± 0.2	118 ± 5	45.6 ± 0.4	0.12 ± 0.01	29 ± 2	37.8 ± 18.5 [a]
CKD-V ($n = 8$)	23.3 ± 0.5 [a]	132 ± 1 [a]	40.4 ± 0.9 [a]	0.27 ± 0.01 [a]	69 ± 4 [a]	21.0 ± 6.8
CKD-T ($n = 8$)	25.0 ± 0.7 [b]	128 ± 4 [b]	41.0 ± 1.8 [b]	0.25 ± 0.01 [b]	68 ± 4 [b]	35.1 ± 9.5 [c]

Data are expressed as mean ± SEM. a: $P < 0.05$ *vs.* Cont-V, b: $P<0.05$ *vs.* Cont-T, c: $P < 0.05$ *vs.* CKD-V. AII: angiotensin II, BUN: blood urea nitrogen, RAWM test: radial arm water maze test, SBP: systolic blood pressure.

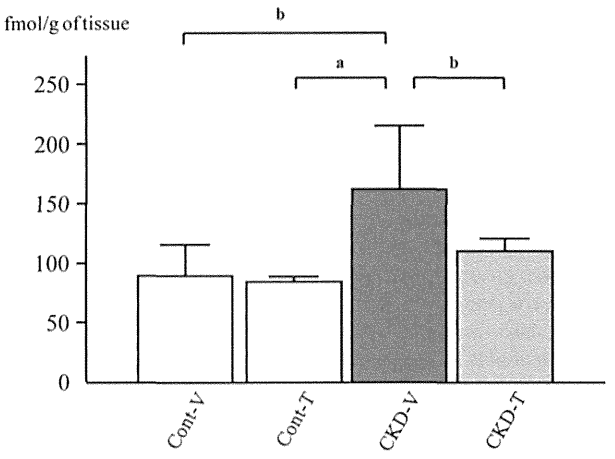

Fig. 1. Angiotensin II concentrations in brain tissue. Concentrations are expressed in femtomoles (fmol) per gram of tissue. Five mice were used in the CONT-V group; six in the CONT-T group; four in the CKD-V group; and six in the CKD-T group. Data are expressed as mean ± SEM. a: $P < 0.01$, b: $P < 0.05$.

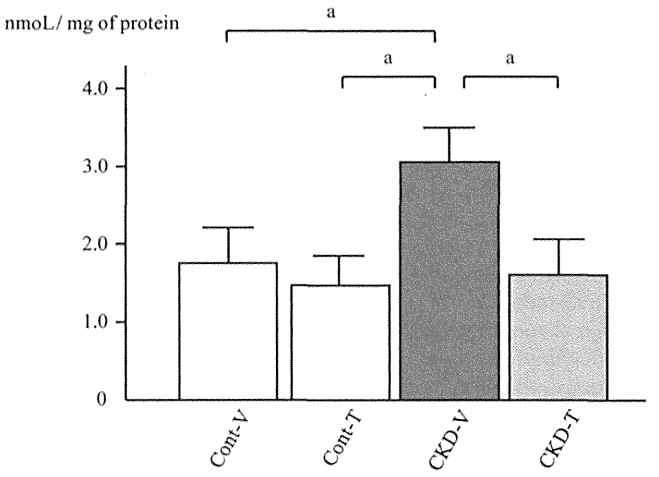

Fig. 3. Malondialdehyde concentrations in brain tissue. Data are expressed as mean ± SEM. a: $P < 0.05$.

(2010) reported that systemic infusion of AII did not affect the amount of brain AII. Therefore, it is thought that brain RAS does not penetrate through a disrupted blood–brain barrier but arises locally in brain tissues. In the present study, local expression of AII increased in the CKD group compared with the control groups; but this expression was suppressed by systemic administration of telmisartan. This result is consistent with findings of the RAWM test, and indicated that brain RAS is a crucial factor of cognitive impairment in CKD. The precise mechanism by which telmisartan prevented the increase of brain AII remains unclear, but we speculate that blockade of AII receptor by telmisartan contributed somehow not only to neurons but also to other brain parenchymal cells to cause a decrease in expression of RAS components in this uremic mouse model (Grobe et al., 2008; Füchtbauer et al., 2011; Zhou et al., 2006).

There are numerous studies examining the role of brain RAS in cognitive dysfunction in experimental models of hypertension and cerebral ischemia (Pelisch et al., 2011; Inaba et al., 2009; Mogi et al., 2006; Tota et al., 2012), and the results suggest that inhibitors of RAS can preserve cognitive function without blood-lowering effects. Pelisch et al. (2011) used Dahl salt-sensitive rats to study increases in brain AII. This model showed disruption of the blood–brain barrier of the hippocampus through elevated brain oxidative stress and cognitive impairment. Similar to our study, olmesartan prevented increases in brain AII and preserved cognitive performance independent of blood pressure. Inaba et al. (2009) reported elevation of oxidative stress in the brain and decreases in cerebral blood flow in chimera mice produced by mating human angiotensinogen transgenic mice with renin transgenic mice. A shuttle avoidance test suggested that the cognitive function of the mice was impaired, but olmesartan preserved their cognitive function and cerebral hemodynamics. These reports suggest that activation of brain RAS has a poor effect on brain physiological functions via oxidative stress.

Telmisartan migrates from the blood circulation to brain parenchyma through the blood–brain barrier, at least in part. Shimizu et al. (2012) reported that radioisotope-labeled telmisartan was distributed in the brain using positron emission tomography. Although we did not compare telmisartan with other AT1 receptor blockers in the present study, numerous *in vivo* studies of non-CKD models have reported similar results using angiotensin receptor blockers other than telmisartan. However, the mechanism via the AT1 receptor to brain parenchymal cells has not yet been determined. In addition, as another specific effect,

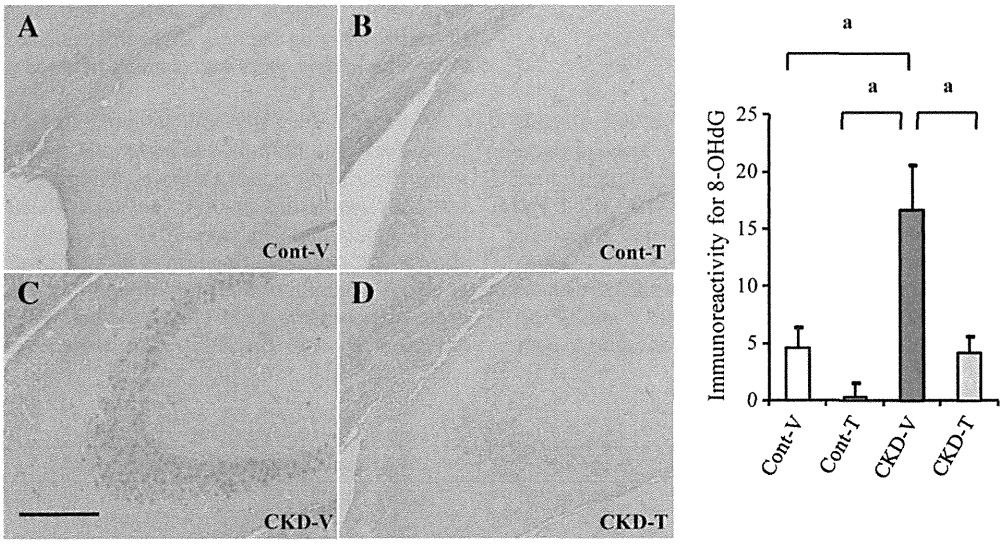

Fig. 2. Immunohistochemical detection of 8-OHdG in the hippocampus. The images on the left show detection of 8-OHdG in the hippocampus (A: a Cont-V mouse, B: a Cont-T mouse, C: a CKD-V mouse, and D: a CKD-T mouse). Scale bar: 200 μm. The graph on the right shows immunoreactivity intensities for each group ($n = 5$). Data are expressed as mean ± SEM. a: $P < 0.01$. 8-OHdG: 8-hydroxy-2'-deoxyguanosine.

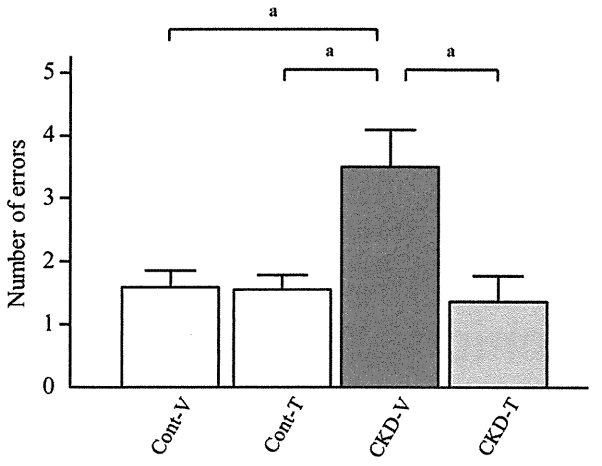

Fig. 4. RAWM test errors. The frequency of errors with RAWM tests during final trials on the 5th day ($n = 8$ in each group). Data are expressed as mean ± SEM. a: $P < 0.05$. RAWM test: radial arm water maze test.

telmisartan has a partial agonistic effect on peroxisome proliferative activator receptor-γ (PPAR-γ). Tsukuda et al. (2009) reported that telmisartan protected cognitive function in a diabetic mouse model. The authors suggested that these results may be attributed not only to blockade of the AT1 receptor, but also activation of PPAR-γ. The present study did not examine the agonistic effect of PPAR-γ, and research on this point is required.

Conclusion

The results of this study suggest that telmisartan has a protective effect against impaired spatial working memory through inhibition of oxidative stress in uremic mice. The origins of brain RAS in CKD remain to be elucidated, and further studies are required to determine the exact pathophysiology of the disease.

Conflicts of interest

The authors declare that there are no conflicts of interest.

Acknowledgments

Telmisartan was kindly supplied by Boehringer Ingelheim Pharma GmbH & Co. KG. (Ingelheim am Rhein, Germany). We are thankful to SRL Inc. for the excellent technical assistance.

References

Acres OW, Satou R, Navar LG, Kobori H. Contribution of a nuclear factor-kappa B binding site to human angiotensinogen promoter activity in renal proximal tubular cells. Hypertension 2011;57:608–13.
Bugnicourt JM, Godefroy O, Chillon JM, Choukroun G, Massy ZA. Cognitive disorders and dementia in CKD: the neglected kidney-brain axis. J Am Soc Nephrol 2013;24:353–63.
Coresh J, Selvin E, Stevens LA, Manzi J, Kusek JW, Eggers P, et al. Prevalence of chronic kidney disease in the United States. JAMA 2007;298:2038–47.
De Deyn PP, Vanholder R, Eloot S, Glorieux G. Guanidino compounds as uremic (neuro) toxins. Semin Dial 2009;22:340–5.
Dong YF, Kataoka K, Toyama K, Sueta D, Koibuchi N, Yamamoto E, et al. Attenuation of brain damage and cognitive impairment by direct renin inhibition in mice with chronic cerebral hypoperfusion. Hypertension 2011;58:635–42.
Dupont AG, Brouwers S. Brain angiotensin peptides regulate sympathetic tone and blood pressure. J Hypertens 2010;28:1599–610.
Elias MF, Elias PK, Seliger SL, Narsipur SS, Dore GA, Robbins MA. Chronic kidney disease, creatinine and cognitive functioning. Nephrol Dial Transplant 2009;24:2446–52.
Etgen T, Sander D, Chonchol M, Briesenick C, Poppert H, Förstl H, et al. Chronic kidney disease is associated with incident cognitive impairment in the elderly: the INVADE study. Nephrol Dial Transplant 2009;24:3144–50.
Füchtbauer L, Groth-Rasmussen M, Holm TH, Løbner M, Toft-Hansen H, Khorooshi R, et al. Angiotensin II Type 1 receptor (AT1) signaling in astrocytes regulates synaptic degeneration-induced leukocyte entry to the central nervous system. Brain Behav Immun 2011;25:897–904.
Fujisaki K, Tsuruya K, Yamato M, Toyonaga J, Noguchi H, Nakano T, et al. Cerebral oxidative stress induces spatial working memory dysfunction in uremic mice: neuroprotective effect of tempol. Nephrol Dial Transplant 2014;29:529–38.
Grobe JL, Xu D, Sigmund CD. An intracellular renin-angiotensin system in neurons: fact, hypothesis, or fantasy. Physiology (Bethesda) 2008;23:187–93.
Hallan SI, Coresh J, Astor BC, Asberg A, Powe NR, Romundstad S, et al. International comparison of the relationship of chronic kidney disease prevalence and ESRD risk. J Am Soc Nephrol 2006;17:2275–84.
Huang C, Johns EJ. Role of brain angiotensin II on somatosensory-induced antinatriuresis in hypertensive rats. Hypertension 2001;37:1369–74.
Inaba S, Iwai M, Furuno M, Tomono Y, Kanno H, Senba I, et al. Continuous activation of renin-angiotensin system impairs cognitive function in renin/angiotensinogen transgenic mice. Hypertension 2009;53:356–62.
Khatri M, Nickolas T, Moon YP, Paik MC, Rundek T, Elkind MS, et al. CKD associates with cognitive decline. J Am Soc Nephrol 2009;20:2427–32.
Kurella-Tamura M, Unruh ML, Nissenson AR, Larive B, Eggers PW, Gassman J, et al. Effect of more frequent hemodialysis on cognitive function in the frequent hemodialysis network trials. Am J Kidney Dis 2013;61:228–37.
Lavoie JL, Cassell MD, Gross KW, Sigmund CD. Localization of renin expressing cells in the brain, by use of a REN-eGFP transgenic model. Physiol Genomics 2004;16:240–6.
Madero M, Gul A, Sarnak MJ. Cognitive function in chronic kidney disease. Semin Dial 2008;21:29–37.
Matsushita K, van der Velde M, Astor BC, Woodward M, Levey AS, de Jong PE, et al. Association of estimated glomerular filtration rate and albuminuria with all-cause and cardiovascular mortality in general population cohorts: a collaborative meta-analysis. Lancet 2010;375:2073–81.
Mogi M, Li JM, Iwanami J, Min LJ, Tsukuda K, Iwai M, et al. Angiotensin II type-2 receptor stimulation prevents neural damage by transcriptional activation of methyl methanesulfonate sensitive 2. Hypertension 2006;48:141–8.
Omata K, Kanazawa M, Sato T, Abe F, Saito T, Abe K. Therapeutic advantages of angiotensin converting enzyme inhibitors in chronic renal disease. Kidney Int 1996;55:S57–62.
Pelisch N, Hosomi N, Ueno M, Masugata H, Murao K, Hitomi H, et al. Systemic candesartan reduces brain angiotensin II via downregulation of brain renin-angiotensin system. Hypertens Res 2010;33:161–4.
Pelisch N, Hosomi N, Ueno M, Nakano D, Hitomi H, Mogi M, et al. Blockade of AT1 receptors protects the blood–brain barrier and improves cognition in Dahl salt-sensitive hypertensive rats. Am J Hypertens 2011;24:362–8.
Saavedra JM. Brain and pituitary angiotensin. Endocr Rev 1992;13:329–80.
Shimizu K, Takashima T, Yamane T, Sasaki M, Kageyama H, Hashizume Y, et al. Whole-body distribution and radiation dosimetry of [11C]telmisartan as a biomarker for hepatic organic anion transporting polypeptide (OATP) 1B3. Nucl Med Biol 2012;39:847–53.
Shimizu H, Saito S, Higashiyama Y, Nishijima F, Niwa T. CREB, NF-κB, and NADPH oxidase coordinately upregulate indoxyl sulfate-induced angiotensinogen expression in proximal tubular cells. Am J Physiol Cell Physiol 2013;304:C685–92.
Tota S, Nath C, Najmi AK, Shukla R, Hanif K. Inhibition of central angiotensin converting enzyme ameliorates scopolamine induced memory impairment in mice: role of cholinergic neurotransmission, cerebral blood flow and brain energy metabolism. Behav Brain Res 2012;232:66–76.
Tsukuda K, Mogi M, Iwanami J, Min LJ, Sakata A, Jing F, et al. Cognitive deficit in amyloid-beta-injected mice was improved by pretreatment with a low dose of telmisartan partly because of peroxisome proliferator-activated receptor-gamma activation. Hypertension 2009;54:782–7.
Unger T, Badoer E, Ganten D, Lang RE, Rettig R. Brain angiotensin: pathways and pharmacology. Circulation 1988;77:I40–54.
Wen CP, Cheng TY, Tsai MK, Chang YC, Chan HT, Tsai SP, et al. All-cause mortality attributable to chronic kidney disease: a prospective cohort study based on 462, 293 adults in Taiwan. Lancet 2008;371:2173–82.
Wilson WL, Roques BP, Llorens-Cortes C, Speth RC, Harding JW, Wright JW. Roles of brain angiotensin II and III in thirst and sodium appetite. Brain Res 2005;1060:108–17.
Zhou J, Pavel J, Macova M, Yu ZX, Imboden H, Ge L, et al. AT1 receptor blockade regulates the local angiotensin II system in cerebral microvessels from spontaneously hypertensive rats. Stroke 2006;37:1271–6.

Hypertension Research (2014) 37, 993–998

www.nature.com/hr

ORIGINAL ARTICLE

Impact of combined losartan/hydrochlorothiazide on proteinuria in patients with chronic kidney disease and hypertension

Kiichiro Fujisaki[1,8], Kazuhiko Tsuruya[1,2,8], Toshiaki Nakano[1], Masatomo Taniguchi[1], Harumichi Higashi[3], Ritsuko Katafuchi[4], Hidetoshi Kanai[5], Masaru Nakayama[6], Hideki Hirakata[7] and Takanari Kitazono[1] on behalf of Impact of Combined Losartan/Hydrochlorothiazide on Proteinuria in Patients with Chronic Kidney Disease and Hypertension (ILOHA) Study Investigators

It is unknown whether the use of diuretics is optimal over other antihypertensive agents in patients with chronic kidney disease (CKD) whose blood pressure remains uncontrolled despite treatment with renin–angiotensin system (RAS) inhibitors. In this study, we assessed the additive effects of hydrochlorothiazide (HCTZ) on reducing proteinuria in CKD patients under treatment with losartan (LS). We conducted a multicenter, open-labeled, randomized trial. One hundred and two CKD patients with hypertension and overt proteinuria were recruited from nine centers and randomly assigned to receive either LS (50 mg, $n=51$) or a combination of LS (50 mg per day) and HCTZ (12.5 mg per day) (LS/HCTZ, $n=51$). The primary outcome was a decrease in the urinary protein-to-creatinine ratio (UPCR). The target blood pressure was $<130/80$ mm Hg, and antihypertensive agents (other than RAS inhibitors and diuretics) were added if the target was not attained. Baseline characteristics of the two groups were similar. After 12 months of treatment, decreases in the UPCR were significantly greater in the LS/HCTZ group than in the LS group. There were no significant differences in blood pressure or the estimated glomerular filtration rate between the two groups. LS/HCTZ led to a greater reduction in proteinuria than treatment with LS, even though blood pressure in the LS group was similar to that in the LS/HCTZ group following the administration of additive antihypertensive agents throughout the observation period. This finding suggests that LS/HCTZ exerts renoprotective effects through a mechanism independent of blood pressure reduction.
Hypertension Research (2014) **37**, 993–998; doi:10.1038/hr.2014.110; published online 26 June 2014

Keywords: angiotensin II type 1 receptor blocker; chronic kidney disease; hydrochlorothiazide

INTRODUCTION

Data from many large-scale clinical trials demonstrate that renin–angiotensin system (RAS) inhibitors such as angiotensin-converting enzyme inhibitor (ACEI) and angiotensin II type 1 receptor blocker (ARB) have an evident effect on kidney protection.[1–5] Recent guidelines on hypertension management[6,7] recommend the concomitant use of several types of antihypertensive drugs when the target blood pressure is not reached. The guidelines recommended the strict control of blood pressure in patients with chronic kidney disease (CKD) with a complication of hypertension; however, the appropriate target value of blood pressure decline is almost never reached using a single RAS inhibitor.

In various combined therapies, the combined use of RAS inhibitors such as ARB or ACEI and calcium channel blocker (CCB) or small amounts of thiazide diuretics has been determined as being effective. However, whether to select CCB or diuretics for concomitant use following RAS inhibitor is clinically an important consideration. The appropriate approach was verified by the GUARD study[8] and the ACCOMPLISH study.[9,10] Subjects of the GUARD study were diabetic nephropathy patients. Subjects of the ACCOMPLISH study were patients at high risk of cardiovascular events. Both studies compared and verified the therapeutic effects when amlodipine (a CCB) or hydrochlorothiazide (HCTZ) (a diuretic) was concomitantly used with ACEI. Although HCTZ reduced albuminuria in both studies,

[1]Department of Medicine and Clinical Science, Graduate School of Medical Sciences, Kyushu University, Fukuoka, Japan; [2]Department of Integrated Therapy for Chronic Kidney Disease, Graduate School of Medical Sciences, Kyushu University, Fukuoka, Japan; [3]Department of Nephrology, St Mary's Hospital, Kurume, Japan; [4]Kidney Unit, National Fukuoka Higashi Medical Center, Koga, Japan; [5]Division of Nephrology, Kokura Memorial Hospital, Kitakyushu, Japan; [6]Division of Nephrology and Clinical Research Institute, Department of Internal Medicine, National Kyushu Medical Center Hospital, Fukuoka, Japan and [7]Division of Nephrology and Dialysis Center, Japanese Red Cross Fukuoka Hospital, Fukuoka, Japan
[8]These authors contributed equally to this work.
Correspondence: Dr K Tsuruya, Department of Integrated Therapy for Chronic Kidney Disease, Graduate School of Medical Sciences, Kyushu University, 3-1-1 Maidashi, Higashi-ku, Fukuoka 812-8582, Japan.
E-mail: tsuruya@intmed2.med.kyushu-u.ac.jp
Received 19 January 2014; revised 18 April 2014; accepted 22 May 2014; published online 26 June 2014

there was also a large decline in the estimated glomerular filtration rate (eGFR). In the ACCOMPLISH study, a significantly large number of cardiovascular events were generated in the HCTZ group, and the renal prognosis was also better in the CCB group. However, only a few patients exhibited overt albuminuria in both studies, and the declining rate of renal function in the patient group was also very slow.

There are no clinical studies to date comparing the effects of diuretics and the other antihypertensive agents on reducing urinary protein under treatment with ARBs and comparable blood pressure control in CKD patients with overt proteinuria. Therefore, we conducted a prospective, randomized, open-labeled, multicenter trial to determine the efficacy of a fixed-dose combination of losartan (LS) plus HCTZ and a normal dose of LS in patients with CKD and hypertension.

METHODS

The present study was a 1-year prospective, randomized, open-labeled, parallel-group, multicenter trial. The objective was to elucidate the renoprotective effects of ARB/low-dose HCTZ combination therapy on CKD patients with proteinuria and hypertension.

The protocol was approved by the Independent Review Board of Kyushu University Hospital (No. 0272) and registered at UMIN-CTR (ID: UMIN000001643). The institutional review boards or ethics committees of all participating institutions approved the study protocol. All patients provided written informed consent.

Study population

Target patients were outpatients with systolic blood pressure (SBP) >130 mm Hg and/or diastolic blood pressure (DBP) >80 mm Hg, or taking antihypertensive drugs at the time when consent was obtained. The following conditions were also required: (1) the urinary protein (mg dl^{-1})/creatinine (mg dl^{-1}) ratio (UPCR) for the 8 weeks before the study commencing exceeded 0.3 (g g^{-1} Cr); (2) eGFR was 15 ml min^{-1} per 1.73 m^2 or more; and (3) patients were aged between 20 and 74 years old. Exclusion criteria were: (1) patients with hepatic dysfunction (e.g., when alanine aminotransferase exceeded the normal upper limit by threefold or more); (2) patients who had a myocardial infarction or apoplexy in the previous 3 months; (3) patients who were or might be pregnant; (4) patients with the possibility of becoming pregnant within the study period and patients who were breastfeeding; (5) patients with a serious nephrotic syndrome (serum albumin <2 g dl^{-1}); (6) immunoglobulin A (IgA) nephropathy patients within a year from commencing steroid therapy; (7) patients with hyperkalemia (5.5 mEq l^{-1} or more); and (8) patients undergoing thiazide diuretics or thiazide-like diuretics administration.

Study design

Eligible patients were randomly assigned in a 1:1 ratio to receive either LS (50 mg per day) or LS (50 mg per day) and HCTZ (12.5 mg per day) combination therapy, each of which was administered once every morning. A 50 mg LS/12.5 mg HCTZ combination tablet was used for combination therapy. On the day of randomization, initial evaluations (medical history and medication), assessments of clinic blood pressure and laboratory tests (blood and urine) were performed after written informed consent was obtained. Figure 1 shows the study design.

ACEI or ARB administered to patients at the time of obtaining consent (-1 M) was changed to LS (50 mg per day). LS (50 mg per day) was additionally administered to patients who were not taking ACEI or ARB. LS (50 mg per day) was continued when allotted to the LS administration group at the time of commencing the allotment drug (0 M), and when allotted to the diuretic administration group, LS was replaced with an LS/HCTZ combination drug. Blood pressure measurements and blood and urine collection were carried out throughout the study period. Antihypertensive drugs other than diuretics, ACEI and ARB, were added when blood pressure did not decline to $<130/80$ mm Hg. Blood pressure measurements and blood and urine collection were carried out at 0, 1, 2, 4, 6 and 12 months following commencement of treatment.

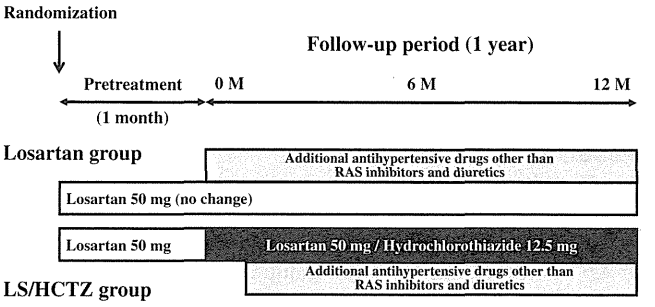

Figure 1 Study protocol. Blood pressure was targeted at $<130/80$ mm Hg during the study period. HCTZ, hydrochlorothiazide; LS, losartan; RAS, renin–angiotensin system.

Adverse events included intractable hypotension symptoms (e.g., fainting or dizziness), hyperkalemia (potassium >6.0 mEq l^{-1}), laboratory data abnormalities (e.g., acute worsening of kidney or liver function) and any side effects that required the discontinuation of medication to protect the patient's best interest.

Measurements

The levels of blood and urinary biochemical parameters and urinary protein excretion were measured in the hospital during consultations as outpatients. All assays were performed using commercially available laboratory equipment. Clinical blood pressure was measured using the auscultation method with a mercury sphygmomanometer after 5 min of rest in a seated position in the hospital. The UPCR was simultaneously estimated using casual urine samples. The eGFR was calculated according to the following formula from the Japanese Society of Nephrology: eGFR (ml min^{-1} per 1.73 m^2) $= 194 \times$ (serum creatinine)$^{-1.094} \times$ age$^{-0.287}$ ($\times 0.739$, if female).[11] CKD was defined as an eGFR <60 ml min^{-1} per 1.73 m^2 and/or the presence of proteinuria.

Study outcome

The primary outcome was determined as the amount of change in the UPCR from the value before commencing treatment to 12 months following commencement of treatment between the two groups. The secondary outcome was the change in blood pressure and eGFR from the value at study commencement to 6 and 12 months following study commencement between the two groups.

Sample size

The planned sample size was 120 cases (60 cases in the LS group and 60 cases in the LS/HCTZ group). With reference to the report by Uzu *et al.*[12] regarding the mean amount of change in urinary protein excretion before and after administration, the difference between CKD patients undergoing administration of ACEI or ARB and those undergoing administration of ACEI or ARB with concomitant use of thiazide was estimated at 0.2 g per day. The standard deviation of the amount of change was surmised to be approximately 0.35 g per day. When a Student's *t*-test was surmised with a difference in mean value of 0.2, standard deviation of 0.35, significance level of 0.05 (two-sided test) and statistical power of 0.80, it was suggested that 50 cases were required for each group. We estimated that 10 to 20% cases would be discontinued/omitted during the study or found to be ineligible following registration, so the target number of cases was set at 60 cases for each group, totaling 120 cases.

Statistical analysis

Statistical analysis was performed using a commercially available software program (JMP statistics 9.0; SAS Institute, Tokyo, Japan). Data are expressed as the mean $\pm$ s.d. or as a percentage. A χ^2 test was applied to examine differences between prevalence in the two treatment groups. Data were analyzed based on the random allocation of participants to the treatment group regardless of the content of subsequent drug administration (intention-to-treat analysis). The

mean value of both groups was compared using a Mann–Whitney *U*-test. Repeated measurement analysis of variance was used to evaluate the therapeutic effect against blood pressure, eGFR and uric acid level. $P<0.05$ was determined to be statistically significant.

RESULTS

Baseline characteristics

In this study, 102 cases (85% of the recommended sample size) satisfying the registration criteria were randomly allocated to the LS group ($n=51$) or the LS/HCTZ group ($n=51$) (Figure 2). Patients' backgrounds of the two groups at baseline are illustrated in Table 1, and there was no significant difference between the groups. In the LS group, three patients undergoing treatment were omitted from the protocol (initiation of hemodialysis: $n=1$; long hospitalization for malignant lymphoma: $n=1$; lost of follow-up: $n=1$), and post-operative follow-up as an outpatient could not be carried out for 12 months. Accordingly, these three patients were excluded as study subjects. In the LS/HCTZ group, seven patients were omitted from the protocol (acute worsening of kidney function: $n=3$; withdrawal of consent: $n=3$; skin eruption: $n=1$). However, it was possible to carry out postoperative follow-up as an outpatient for 12 months for all seven patients. Therefore, all 51 patients were included as study subjects.

The drugs taken during the study are shown in Table 2. In the losartan group, there were many cases in which CCB was additionally administered during the course, and the rate of internal use of CCB was significantly higher compared with the LS/HCTZ group.

Changes in clinical blood pressure

There were no differences in SBP or DBP between the two groups during the treatment period (Figure 3). SBP was 125.2 ± 13.3 mm Hg in the LS group and 124.9 ± 15.3 mm Hg in the LS/HCTZ group; DBP was 73.0 ± 9.4 mm Hg in the LS group and 74.1 ± 8.6 mm Hg in the LS/HCTZ group at 12 months following the commencement of treatment, with no significant difference between the two groups. The ratio of patients with blood pressure $<130/80$ mm Hg following 12 months was 50% in the LS group and 47% in the LS/HCTZ group, with no significant difference between the two groups.

Changes in the UPCR

At 6 and 12 months following commencement of the study, the amount of the UPCR decline in the LS/HCTZ group was significantly greater than that in the LS group (6 M: 0.21 ± 0.99 *vs.* $-0.54\pm0.73\,g\,g^{-1}$ Cr, $P<0.05$; 12 M: 0.02 ± 0.76 *vs.* $-0.55\pm0.71\,g\,g^{-1}$ Cr, $P<0.05$) (Figure 4a). The relationship between BP reduction and the reduction in proteinuria is not significantly (Figures 4b and c).

Changes in eGFR and uric acid

The eGFR declined slightly more in the LS/HCTZ group compared with the LS group at 6 and 12 months following commencement of treatment; however, there was no significant difference between the two groups (6 M: LS $46.1\pm23.5\,ml\,min^{-1}$ per $1.73\,m^2$, LS/HCTZ $39.6\pm21.1\,ml\,min^{-1}$ per $1.73\,m^2$; 12 M: LS $45.0\pm23.3\,ml\,min^{-1}$ per $1.73\,m^2$, LS/HCTZ $40.5\pm21.7\,ml\,min^{-1}$ per $1.73\,m^2$) (Figure 5). The uric acid level following 12 months was significantly higher in the LS/HCTZ group (6.3 ± 1.3 *vs.* $7.1\pm1.4\,mg\,dl^{-1}$, $P<0.05$) (Figure 6).

DISCUSSION

The results of this study showed that combination therapy with LS/HCTZ led to a greater reduction in proteinuria than treatment with LS alone at the same blood pressure level. This study is the first to provide evidence to support the efficacy of LS/HCTZ combination therapy in patients, independent of antihypertensive effects. This finding suggests that the addition of diuretics constitutes an optimal treatment for patients with CKD under treatment with ARBs and that diuretics exert renoprotective effects through a mechanism independent of blood pressure reduction.

In addition to RAS inhibition, it is believed that strict blood pressure control has a major role in preventing the progression of renal disease.[7,13,14] In this study, there was no difference between SBP and DBP in the two groups, with the average reaching the target blood pressure. In addition, there was no significant difference in the eGFR of both groups throughout the observational period of 1 year.

The following three points may be considered for the mechanism by which LS/HCTZ exhibited a urinary protein reducing effect in this study. The first point is the declining effect on blood pressure with

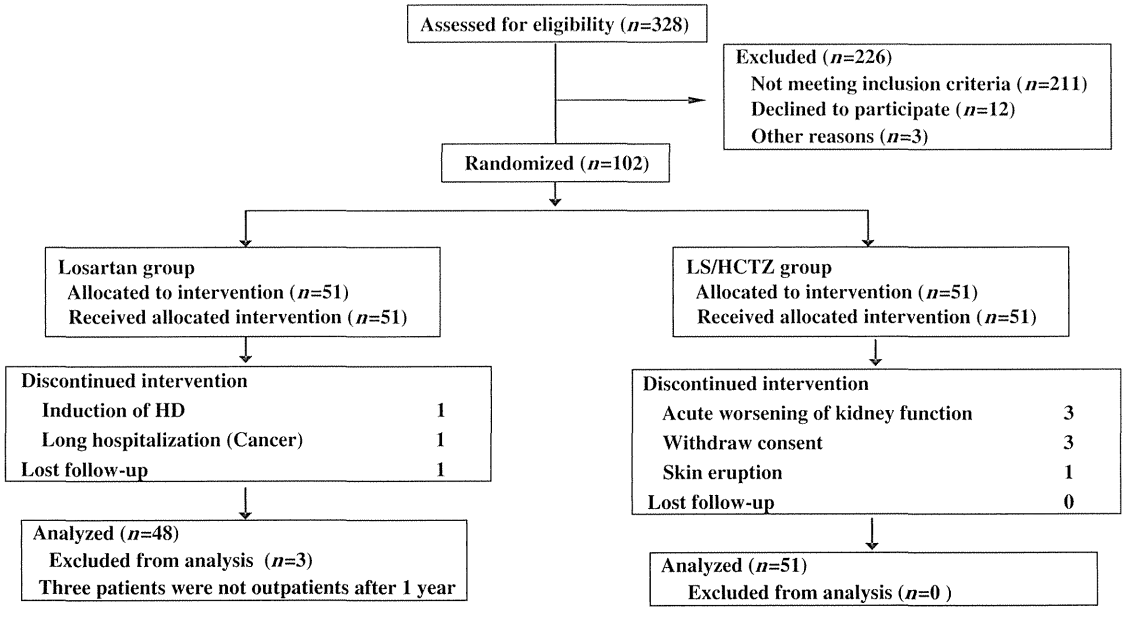

Figure 2 Flow chart of patient enrollment and follow-up. HCTZ, hydrochlorothiazide; HD, hemodialysis; LS, losartan.